

REVIEW

Open Access



Mechanism, Actuation, Perception, and Control of Highly Dynamic Multilegged Robots: A Review

Jun He and Feng Gao*

Abstract

Multilegged robots have the potential to serve as assistants for humans, replacing them in performing dangerous, dull, or unclean tasks. However, they are still far from being sufficiently versatile and robust for many applications. This paper addresses key points that might yield breakthroughs for highly dynamic multilegged robots with the abilities of running (or jumping and hopping) and self-balancing. First, 21 typical multilegged robots from the last five years are surveyed, and the most impressive performances of these robots are presented. Second, current developments regarding key technologies of highly dynamic multilegged robots are reviewed in detail. The latest leg mechanisms with serial-parallel hybrid topologies and rigid-flexible coupling configurations are analyzed. Then, the development trends of three typical actuators, namely hydraulic, quasi-direct drive, and serial elastic actuators, are discussed. After that, the sensors and modeling methods used for perception are surveyed. Furthermore, this paper pays special attention to the review of control approaches since control is a great challenge for highly dynamic multilegged robots. Four dynamics-based control methods and two model-free control methods are described in detail. Third, key open topics of future research concerning the mechanism, actuation, perception, and control of highly dynamic multilegged robots are proposed. This paper reviews the state of the art development for multilegged robots, and discusses the future trend of multilegged robots.

Keywords: Multilegged robot, Mechanism, Actuation, Perception, Control

1 Introduction

Autonomous robotic systems may be classified into three major areas: 1) less inputs–single end-effector–less outputs (LSL) robotic systems such as wheeled and tracked vehicles, 2) multiple inputs–single end-effector–multiple outputs (MSM) robotic systems such as autonomous mobile robots (AMRs) with manipulators, and 3) multiple inputs–multiple end-effectors–multiple outputs (MMM) robotic systems. Legged robots are typical MMM robotic systems. For example, a hexapod robot with three-degrees-of-freedom (3-DOF) legs has 18

inputs, one body end-effector and six leg end-effectors, and 42 outputs. More than 50% of the earth's surface is inaccessible to traditional vehicles with wheels or tracks. Compared to their LSL and MSM counterparts, legged robots possess superior mobility in natural, irregular terrain. However, to further expand their capabilities, legged robots require more complicated mechanisms and control modes.

In this paper, the term “highly dynamic multilegged robots” refers to all quadruped and hexapod walking robots with dynamic stabilities, capable of running, jumping, and hopping while maintaining self-balance against sliding or external impacts. These robots have recently shown impressive advancements in terms of dynamic capabilities with the aid of various novel actuation and control strategies, yielding dynamic

*Correspondence: fengg@sytu.edu.cn

State Key Laboratory of Mechanical System and Vibration, School of Mechanical Engineering, Shanghai Jiao Tong University, Shanghai 200240, China

performance comparable to human beings or other mammals. For instance, the MIT Cheetah 2 quadruped robot can avoid sudden obstacles by jumping [1], and its bounding speed reaches up to 6.4 m/s [2]. Another impressive example is the ANYmal quadruped robot, which exploits a sim-to-real strategy: first, reinforcement learning is used for training neural network policies in the simulated virtual irregular environment; next, the obtained policies are transferred to the ANYmal quadruped robot. In this way, ANYmal achieves high-level locomotion skills, higher speeds than ever before, and the capability of recovering rapidly from falling [3]. Compared to quadruped robots, hexapod legged robots have better stability and higher payload capacity owing to their tripod gaits, making them suitable for disaster-rescue tasks. For example, the Crabster hexapod robots, developed for the exploitation of ocean resources, are capable of seabed walking and carrying out underwater tasks [4]. Shortly after the Fukushima Daiichi disaster in March 2011, some mobile robots such as iRobot and Quince entered the nuclear power plant and carried out inspections and simple operations. However, these robots failed quickly because of high radiation. It is now widely acknowledged that robotic technologies at that time were far from sufficient for carrying out complex rescue operations [5]. Recently, supported by the National Basic Research Program of China (973 Program), a series of hexapod robots with parallel legs were developed by Shanghai Jiao Tong University (SJTU) for firefighting, transportation, and detection in disaster environments, such as nuclear accidents [6–8]. The payloads of these hexapod robots can reach up to 500 kg. In the DARPA Robotics Challenge held in 2015, many humanoid robots successfully performed various rescue operations, such as driving a car, cutting a pipe, and opening a door in a simulated disaster scenario of a nuclear power plant [9]. These new-generation legged robots featured high-level force and vision perception systems, enabling force control and obstacle avoidance.

Despite the great advances made thus far, the compliance, agility, and robustness of multilegged robots are still significantly worse than their biological counterparts [10]. Therefore, legged robots have seldom been used for commercial applications. In fact, robustness and safety are the key considerations for legged robots in outdoor environments, easily outweighing agility and autonomy. In practice, it is very difficult for current legged robots to be used in real applications in outdoor environments [11]; actually, only a few legged robots take into account the requirements of a specific application, such as nuclear disaster relief (e.g., SJTU hexapod robots [6–8]) or inspection of gas and oil sites (e.g., ANYmal [3] and its previous version). In addition, the performances

of legged robots are related to many factors, including their mechanisms and actuation, perception, and control methods. Hence, it is necessary to survey the evolution of these technologies.

This paper reviews recent advances in highly dynamic multilegged robots with respect to their mechanisms and actuation, perception, and control strategies. The rest of this paper is organized as follows. In Section 2, we survey the most significant multilegged robots reported in the last five years. A review of previous multilegged robots can be found in Refs. [12–14]. Sections 3–6 discuss the mechanisms and actuation, perception, and control technologies of highly dynamic multilegged robots, respectively. In Section 7, based on the findings of the previous sections, key open topics for future research are proposed. Lastly, conclusions are addressed in Section 8.

2 Recent Multilegged Robots

2.1 Quadruped Robots

2.1.1 HyQ2Max and HyQreal

The first HyQ robot, developed by Istituto Italiano di Tecnologia (IIT) in 2011, was a fully hydraulic, torque-controlled quadruped robot capable of running and jumping [15]. HyQ2Max, pictured in Figure 1(a), is an improved

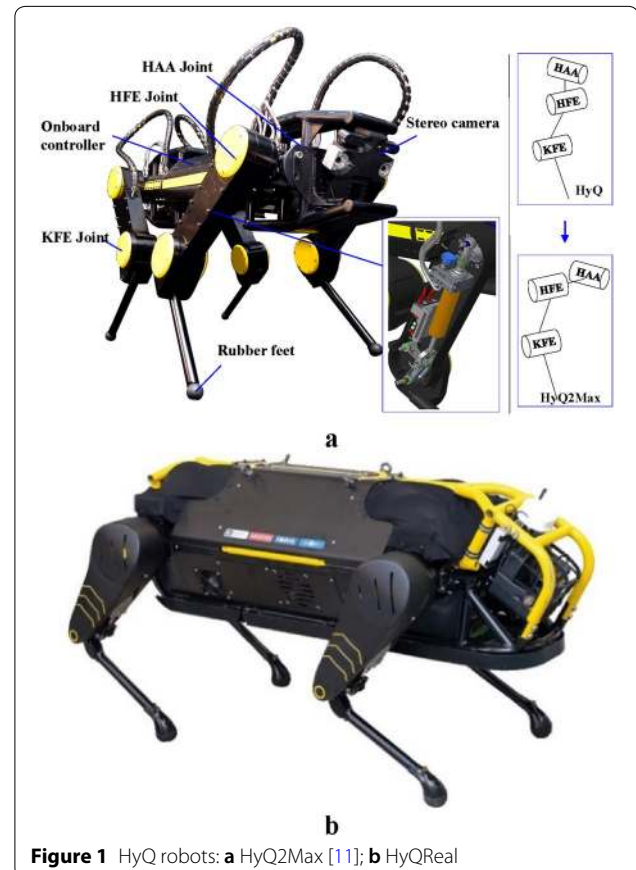


Figure 1 HyQ robots: **a** HyQ2Max [11]; **b** HyQReal

version with joint torque and range much larger than those of the previous version. All electronic devices such as sensors, valves, and actuators are protected inside the mechanical structure to improve the robot's reliability and robustness against impacts and dirt. Both the torso and leg structures are made of strong aerospace-grade aluminum alloy. The outline dimensions of HyQ-2Max are approximately $1.306 \text{ m} \times 0.544 \text{ m} \times 0.918 \text{ m}$ (length \times width \times height), and its weight is about 80 kg (off-board power) [16]. For each leg, there is a hip abduction/adduction (HAA) joint, a hip flexion/extension (HFE) joint, and a knee flexion/extension (KFE) joint. The HAA and HFE joints are rotary hydraulic actuators. The KFE joint is actuated by a four-bar linkage mechanism with a hydraulic cylinder. The ranges of the HAA, HFE, and KFE joints are respectively 80° , 270° , and 165° [11]. The maximum speeds on rough terrain and flat ground are 0.5 m/s and 1.5 m/s, respectively [17]. The step height and depth for stair climbing are respectively 0.12 m and 0.3 m [18]. To perform a self-righting motion, the flexion/extension plane of the leg is placed outward with respect to the HAA axis, which is different from the leg configuration of HyQ, as seen in Figure 1(a). Each joint has a high-resolution absolute encoder and torque sensors. Owing to the EtherCAT real-time communication, the position and torque control of all joints can be carried out at a frequency of 1 kHz [19].

Recently, at the International Conference of Robotics and Automation (ICRA 2019), IIT presented the latest version of the HyQ quadruped robot, called HyQReal, which is capable of pulling a small passenger airplane for more than 10 m, as seen in Figure 1(b) (cited from dls.iit.it). The robot is 1.33 m long, 0.9 m tall, and weighs 130 kg. Compared to its predecessors, HyQReal quadruped robot is completely power-autonomous, with on-board hydraulics, batteries, and wireless communication. In addition, HyQReal is protected by an aluminum roll cage

and skin made of Kevlar, glass fiber, and plastic. The technical specifications of HyQ2Max and HyQReal are shown in Table 1.

2.1.2 StarLETH and ANYmal

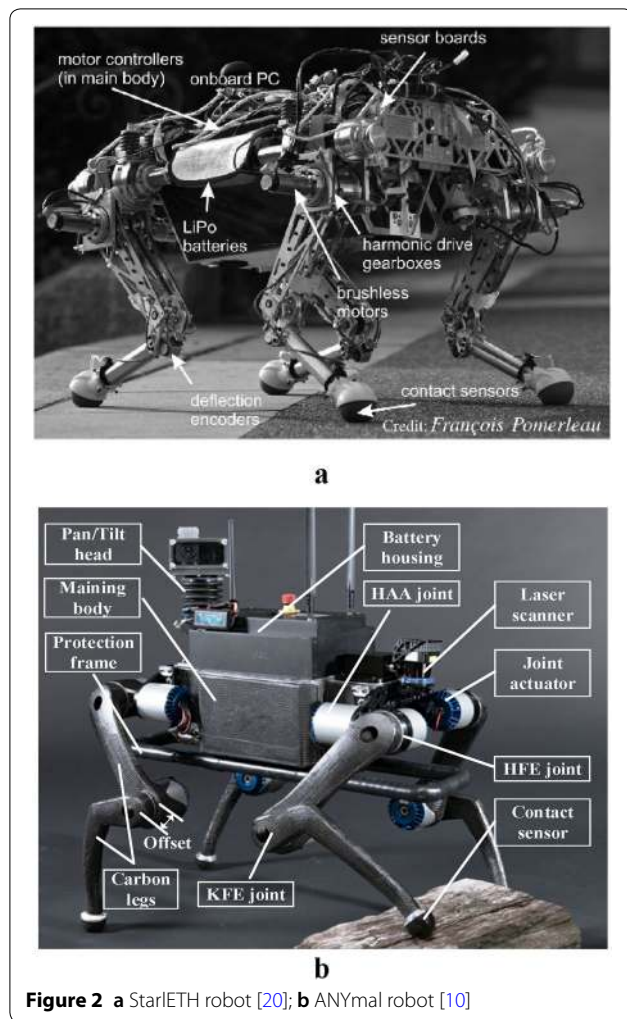
The ANYmal quadrupedal platform [10] was specifically developed for autonomous operation in challenging environments. Its predecessor StarLETH [20] was designed to participate in the ARGOS (Autonomous Robot for Gas and Oil Sites) Challenge for the inspection of petrochemical facilities. In this challenge, each robot has to navigate in a multilevel, outdoor facility, examine checkpoints, and detect, identify, and report internal and external anomalies. The leg links of ANYmal are installed with an offset so that the KFE joint can rotate with a range of nearly 360° , as seen in Figure 2. Thus, the four legs of the robot can be folded and change their configurations. The outline dimensions in the standing state are approximately $0.8 \text{ m} \times 0.6 \text{ m} \times 0.7 \text{ m}$ (length \times width \times height), whereas the height in the lying state is only 0.4 m. The weight of ANYmal is only 30 kg, its payload can be up to 10 kg, and it can reach a speed of up to 3.6 km/h. Thanks to this high mobility, ANYmal can use its feet to open a door or surmount obstacles. Excellent joint mobility also allows the robot to climb stairs, get across obstacles without touching them, and change body height and orientation for inspection. ANYmal obtains its excellent locomotion skills via machine learning. For example, it is capable of learning how to run in unstructured environments, get up after a fall, and precisely follow desired body trajectories [3].

2.1.3 MIT Cheetah

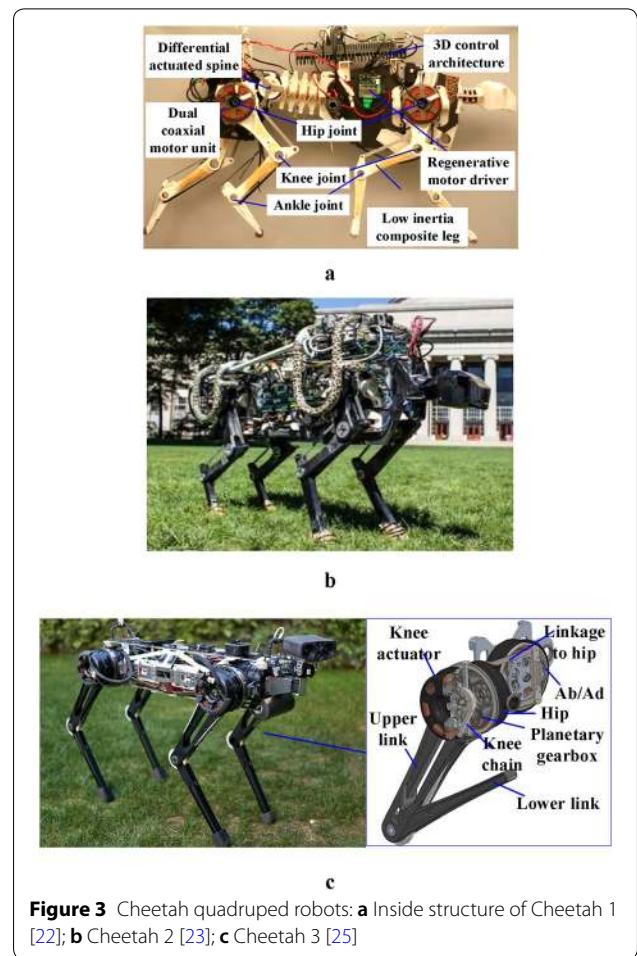
The Massachusetts Institute of Technology (MIT) presented a series of high-performance quadruped robots, called Cheetah 1 through 3, which can be seen in Figure 3. Cheetah 1 has a maximum speed of 6 m/s. Its

Table 1 Specifications of HyQ2Max and HyQReal [11, 15, 16]

Specifications	HyQ2Max	HyQReal
Weight (kg)	80	130
Length \times width \times height (m)	$1.306 \times 0.544 \times 0.918$	$1.33 \times 0.67 \times 0.9$
DOFs of leg	3	3
Ranges of HAA, HFE, and KFE ($^\circ$)	80, 270, 165	–
Torques of HAA, HFE, and KFE (N·m)	120, 245, 250	165, 200, 225
Upper, lower leg segment lengths (m)	0.36, 0.38	0.36, 0.38
Maximum speed (m/s)	1.5	–
Computers	–	2, Vision & control
Hydraulic pumps	–	2, Front & hind legs
Perception	–	Lidar, RGB-D



mass is 39.406 kg, and the total cost of transport (COT [21]) is 0.51 [22]. Cheetah 2, presented in 2015, can use a bounding gait to obtain the maximum speed of 6.4 m/s [23]. The COT of Cheetah 2 is 0.47, smaller than that of Cheetah 1. The leg configuration of Cheetah 2 is a planar serial mechanism. The knee joint is actuated by a linkage mechanism, and thus its actuator can be assembled on the hip. Each leg also has a passive flexible ankle joint. Furthermore, Cheetah 1 has a flexible spine, which uses a differential gear to connect to the rear hip joints. The spine stiffness acts as a parallel spring, which is able to store and release potential energy during movement [24]. Recently, Bledt et al. [25] presented Cheetah 3. Compared to its predecessors, the abduction/adduction DOF is added to the hip joint. The weight of Cheetah 3 is 45 kg, and its outline dimensions are about 0.6 m × 0.256 m × 0.2 m (length × width × height). The robot has 0.45 kWh onboard batteries that provide approximately a two-hour



runtime. The lowest COT of Cheetah 3 is 0.45 during trotting [25].

2.1.4 SCalf-II, HIT, Baby elephant, and CNVI Robots

In 2013, supported by the National High Technology Research and Development Program (863 Program) of China, Shandong University (SDU), the National University of Defense Technology (NUST), the Harbin Institute of Technology (HIT), the Beijing Institute of Technology (BIT), and Shanghai Jiao Tong University (SJTU) developed five hydraulic highly dynamic quadruped robots, as seen in Figure 4(a)–(c). In recent years, these robots have continued to obtain advances in the fields of dynamic locomotion and control.

The SCalf-II robot [26] was developed by SDU. Each leg of this robot has three active DOFs and one passive DOF. It can trot in unstructured terrain using compliant control, and it has the capability of self-balancing after side impact. SJTU’s Baby elephant robot adopts a hybrid leg configuration. The HAA joint is connected to the body frame in series, whereas both the HFE and KFE

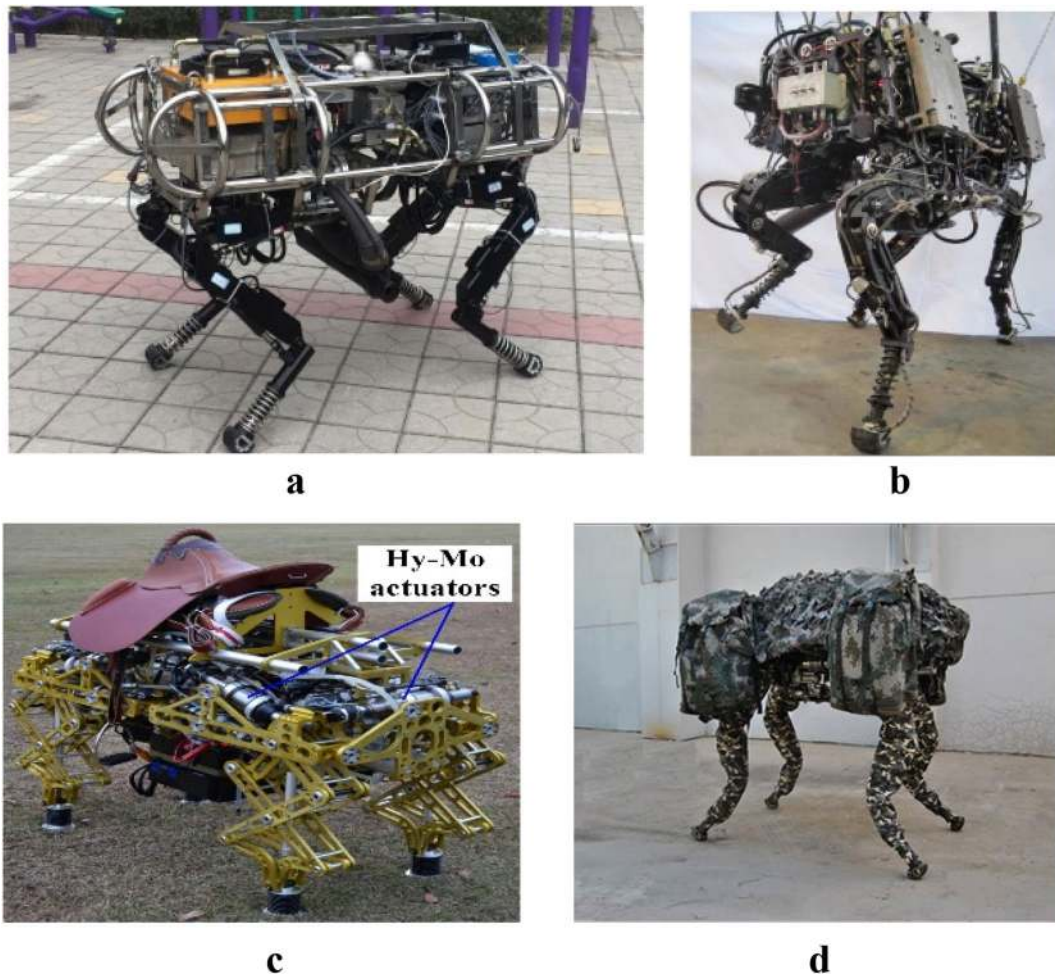


Figure 4 Hydraulic quadruped robots: **a** SDU SCalf-II; **b** HIT robot; **c** SJTU Baby elephant; **d** CNVI quadruped robot

joints are realized by a special parallel mechanism. Compared to its serial or parallel counterparts, the hybrid mechanism can support a bigger payload and has a larger workspace. In addition, there are three passive DOFs on the ankle, which enables the robot to adapt to complex ground environments very well. A novel motor-combined hydraulic actuator called “Hy-Mo” was designed to actuate the joints. The electrical motor controls the screw valve inside the cylinder to obtain the given motion, while the output power of the cylinder is provided by the hydraulic pump. Each Hy-Mo actuator can provide a push or pull force of up to 7500 N. Compared to the traditional hydraulic system, there are no servo-valves, accumulators, filters, or coolers for the Hy-Mo actuation system.

Recently, the China North Vehicle Institute (CNVI) also developed a hydraulically actuated quadruped robot (cited from noveri.norincogroup.com.cn). The robot was designed to perform difficult tasks, such as

transportation and detection in mountainous areas. The detailed specifications of SCalf-II, HIT [27], SJTU Baby elephant [28], and CNVI quadruped robots are shown in Table 2.

2.1.5 SPOT Mini, Laikago, Jueying, and Other Electric Quadruped robots

Some versatile legged robots, such as Spot Mini (launched in July 2019), Laikago (in May 2019), and Jueying (in November 2019), have been made commercially available. These robots might lead to breakthroughs in the translation of more legged robots from laboratory to market as developers aim to create competitive products.

Spot Mini. The Spot Mini quadruped robot developed by Boston Dynamics is shown in Figure 5(a) (cited from www.bostondynamics.com). The SPOT Mini robot can climb stairs and traverse rough terrain with unprecedented ease. The trotting speed reaches up to 1.6 m/s, and the payload capacity is about 14 kg. Boston Dynamics

Table 2 Specifications of SCalf-II, HIT, SJTU, and CNVI quadruped robots [26–28]

Specifications	SCalf-II	HIT	SJTU	CNVI
Length × width × height (m)	1.1 × 0.49 × 1	–	1.2 × 0.5 × 1	1.2 × 0.7 × 1
Weight (kg)	123	150	130	130
Payload (kg)	120	52	50	50
Max speed (km/h)	5	4.32	3.74	6
Gaits	Trot Hopping Creep	Trot Creep	Trot Creep	Trot
Active DOFs	3	3	3	3
Passive DOFs	1	1	3	–
Running time (min)	40	40	40	120
Slope (°)	10	10	10	30
Obstacle height (mm)	150	150	150	–

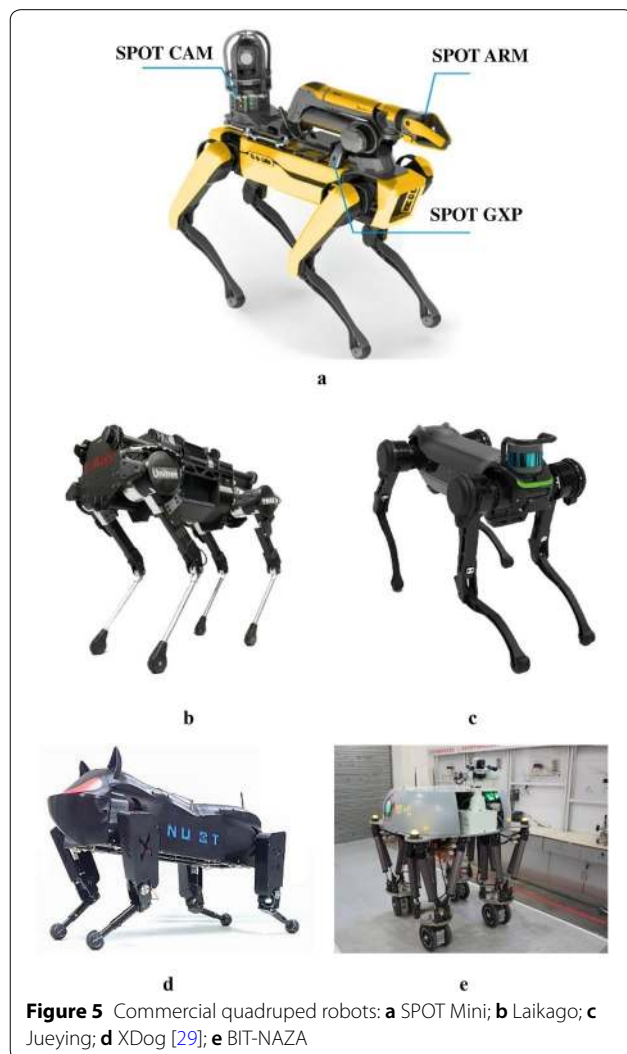


Figure 5 Commercial quadruped robots: **a** SPOT Mini; **b** Laikago; **c** Jueying; **d** XDog [29]; **e** BIT-NAZA

built the robot to be a rugged and customizable platform that can meet industrial sensing and remote operation needs. The customized features and capabilities can be easily embedded in the control system through the client library. The user can select the poses and velocities of the robot using customized application programs, and the software platform of Spot Mini provides access to vision navigation. Therefore, the application program can access the perception data. Recently, Boston Dynamics launched the latest SPOT Mini robot, which contains one arm, one SPOT CAM system, and an additional power source. The arm has six DOFs and its payload is 4 kg. The arm can be used to open doors and manipulate objects. The SPOT CAM includes a color feed and one optional pan-tilt-zoom camera, providing the robot with better situational awareness. The additional power source provides regulated power and an Ethernet breakout for easy attachment of custom and third-party payloads.

Laikago. The Laikago quadruped robot, shown in Figure 5(b), was developed by Unitree Robotics (cited from www.unitree.cc). It was designed to help normal people with tasks like carrying objects or to act as a companion. Each leg has three DOFs, and thus the whole robot has 12 high-performance motors. The weight of the robot with the battery is about 22 kg. The payload is more than 9 kg, the outline dimensions are about 0.55 m × 0.35 m × 0.6 m (length × width × height), the maximum speed is 1.4 m/s, and the maximum climbing slope is more than 20°. The robot is very stable, and it can remain stable on uneven surfaces and when kicked. Its successor, the Aliengo quadruped robot, can even carry out very daunting tasks, such as doing a backflip.

Jueying. The Jueying quadruped robot, pictured in Figure 5(c), was developed by Deep Robotics (cited from www.deeprobotics.cn). The weight of the robot is 40 kg, the maximum payload is 10 kg, the outline dimensions

are $0.85 \text{ m} \times 0.5 \text{ m} \times 0.65 \text{ m}$ (length \times width \times height), and the maximum speed is more than 7 km/h. This robot can perform trotting and galloping gaits, and it can run and jump on unstructured terrains. Since the control period is approximately 0.5 ms, the robot can adapt quickly to unexpected disturbances such as contact collisions. It is also capable of adjusting the position and pose of the torso to avoid falling down. Moreover, the jumping robot has great versatility and can carry out some complicated tasks such as heading a ball and jumping through a ring of fire.

In addition, there are other electric quadruped robots in China. For example, the National University of Defense Technology developed a small electric quadruped robot, XDog [29], as seen in Figure 5(d). The XDog's weight without the battery is about 15 kg. The outline dimensions are about $0.4 \text{ m} \times 0.3 \text{ m} \times 0.3 \text{ m}$ (length \times width \times height). Each leg has three active DOFs and one passive prismatic DOF. The parallel mechanism is used for the design of the electric quadruped robot. Furthermore, the Beijing Institute of Technology developed a leg-wheel robot with parallel legs, named BIT-NAZA, which is pictured in Figure 5(e) (cited from www.bit.edu.cn). Each leg is a 6-DOF parallel Stewart platform. Its walking speed is about 4 km/h. Owing to the high stiffness of parallel legs, the ratio of the payload to the weight reaches up to 1.875, which is much greater than other electronic quadruped robots with serial legs.

2.2 Hexapod Robots

2.2.1 Lauron-V

The Lauron-V hexapod walking robot developed by the FZI Research Center for Information Technology is shown in Figure 6. Its outline dimensions are $0.9 \text{ m} \times 0.8 \text{ m} \times 0.84 \text{ m}$ (length \times width \times height), its weight is 42 kg with the batteries, and its maximum payload is approximately 10 kg. Table 3 shows the main

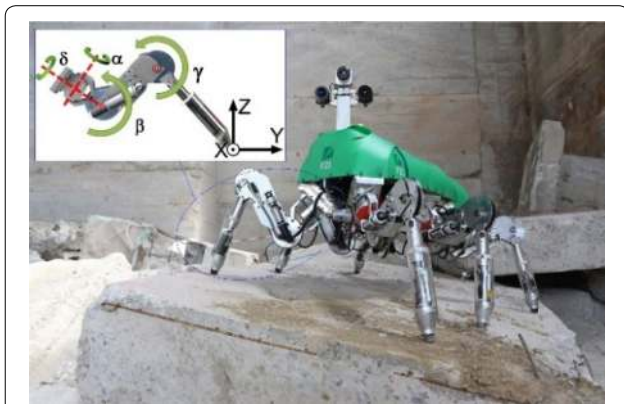


Figure 6 The Lauron-V hexapod robot [30]

Table 3 The technical specifications of Lauron-V [30, 31]

Class	Specifications
No. of Joints per Leg	4 (delta, alpha, beta, gamma)
No. of Head Joints	2 (pan & tilt)
Total DOF (active)	26
Compliance	Spring damper in each foot (6 passive DOF)
Size [footprint]	$0.9 \text{ m} \times 0.8 \text{ m}$
Height [min–max]	$0.61 \text{ m}–0.84 \text{ m}$ (form ground to PTU head)
Weight	40 kg (+ 2 kg for batteries)
Max Payload	10 kg
Power Supply	> 2 h with $2 \times 22.2 \text{ V } 8 \text{ Ah}$ (LiPo)
Power Consumption	Standing: 100 W, Walking 150 W
On-board PC	Intel Core i7 4 \times 3.0 GHz with 8 GB RAM
Modular Sensors	IR-Camera, Stereo-Camera, RGB-D, Velodyne HDL-32E, Rotating Hokuyo

technical specifications of Lauron-V. Compared to its previous versions, Lauron-I through Lauron-IV, each leg of Lauron-V has an additional (fourth) rotational joint. Therefore, the robot can change the pose of any of its feet to optimize the load distribution [30]. In addition, each leg has a passive DOF with a spring damper. The Lauron-V robot can traverse large obstacles with a slope larger than 25° and maintain its balance on an incline of 43° [31]. The robot is also able to manipulate objects with its two front legs. The Lauron robot has a behavior-based control system, which enables the robot to walk in unstructured environments without accurate planning.

2.2.2 Crabster 200

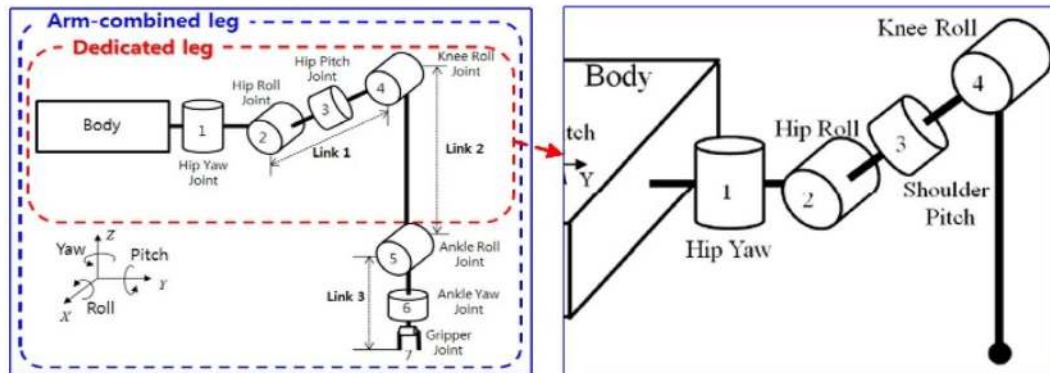
The Crabster200 hexapod walking robot was developed by the Korea Institute of Ocean Science and Technology (KIOST) for seabed surveying and underwater precision work in coastal areas. The Crabster200 robot is able to resist hydraulic pressure of up to 25 bar. The robot is $2.42 \text{ m} \times 2.45 \text{ m} \times 1.16 \text{ m}$ (length \times width \times height). The weight of the robot is approximately 300 kg, and it has a maximum speed of 0.5 m/s. There are two 7-DOF arm-combined legs and four 4-DOF dedicated legs as shown in Figure 7 [32]. Table 4 gives the technical specifications of Crabster200 [32, 33]. The geometrical parameters of each leg were designed according to biological data of crabs. Moreover, each leg has an additional shoulder pitch joint so that the body posture can be adjusted to adapt to creep inclines and to optimize the load distribution in a shallow sea with high tidal current.

2.2.3 Octopus, Hexabot-IV, and HIT Hexapod Robots

Pictured in Figure 8, both the Octopus [34] and Hexabot-IV [6] hexapod robots with high payloads were developed by Shanghai Jiao Tong University for daily maintenance



a



b

Figure 7 **a** The Crabster200 hexapod robot [32]; **b** arm-combined leg mechanism [33]

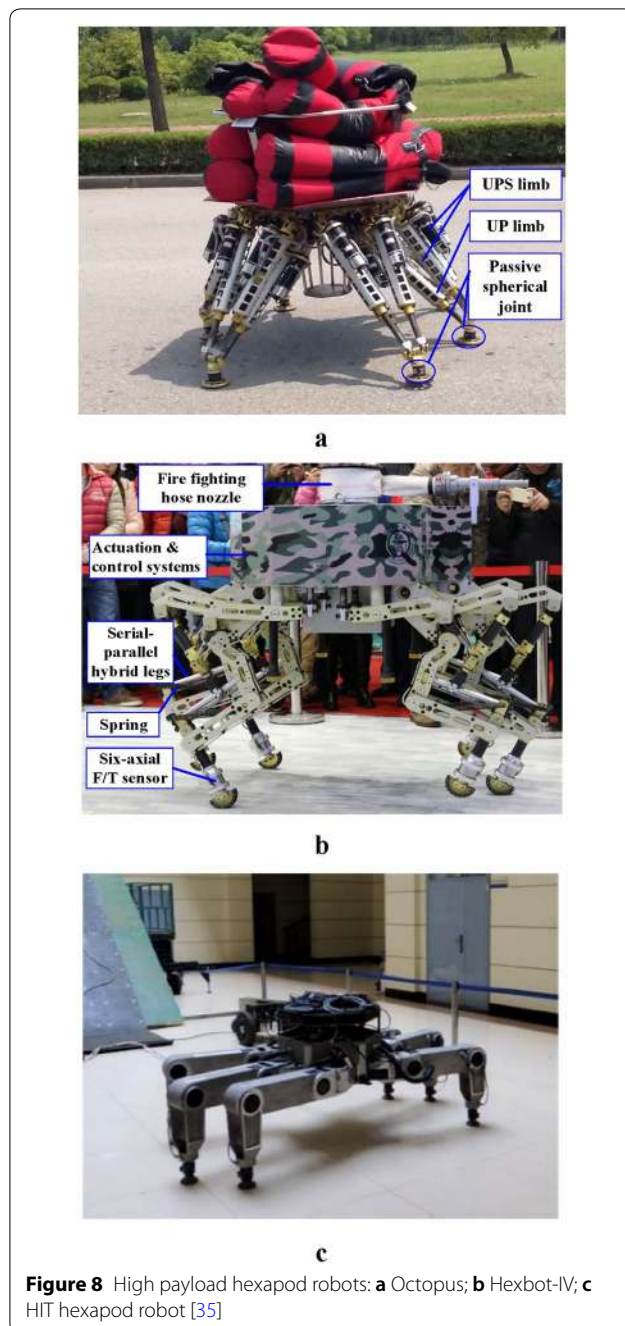
Table 4 Specifications of CR200 [32, 33]

Class	Specifications
Overall size	2.42 m (L) × 2.45 m (W) × 1.16 m (H)
Weight	300 kg
Max. ground clearance	Higher than 0.5 m
Number of legs	Four 4-DOF legs and two 7-DOF legs with grippers
Max. walking speed	0.5 m/s
Max. depth of water	200 m
Max. endurable tidal current	2 knots
Power supply	External power via cable

and emergency relief of nuclear power plants. Compared to quadruped walking robots, hexapod robots can accept higher payloads and achieve greater stability, which facilitates operation and transportation in unstructured environments. Each leg of the Octopus robot is a 3-DOF parallel mechanism. There is a passive spherical joint in

the ankle of each leg. The parallel mechanism has one universal-prismatic (UP) limb and two universal-prismatic-spherical (UPS) limbs. Three prismatic pairs are active joints. The whole robot is a double parallel structure, which provides high load capacity, load-to-weight ratio, and stiffness. Moreover, the robot body is isotropic, which gives it high kinematic dexterity and good obstacle avoidance. Its weight is about 200 kg, and the maximum payload of the robot is more than 500 kg. The maximum climbing slope is approximately 25°, and it can traverse obstacles with a height of up to 400 mm.

The Hexabot-IV [6] is a hexapod walking robot intended to carry rescue equipment such as firefighting hose nozzles, electric drills, or manipulators. Its outline dimensions are about 1.1 m × 0.72 m × 1 m (length × width × height) in the standard standing position. The weight of the Hexabot-IV is 270 kg with two sets of battery packages, the maximum payload is more than 50 kg, and the speed reaches up to 0.54 m/s. To lower the leg inertia, a parallel mechanism



(PM) is employed to indirectly move the leg tip in three dimensions. The upper part of the leg mechanism is a PM with three limbs: a revolute-universal (RU) limb and two revolute-universal-spherical (RUS) limbs. The lower part is a spatial multilinkage mechanism. Thus, the leg has a serial-parallel hybrid mechanism. Furthermore, both the actuation and control systems are located in the body frame and are well protected from harsh environments.

The HIT hexapod robot [35], pictured in Figure 8(c), was designed to perform transportation and perception tasks on the lunar surface. The RRRS serial configuration is adopted for the leg. Each leg has three active DOFs and a passive spherical joint on the ankle joint. The ratio of the payload to the weight is 0.46. The robot can walk using crab-type, ant-type, and mixture-type gaits.

3 Mechanism

Similar to the skeletal system of mammals, the mechanisms of multilegged robots determine the basic properties of the robotic system, such as mobility, workspace, and singularity. The biological bone system has inspired the mechanism design of many multilegged robots. A biological configuration may lead to large amounts of kinematic mechanisms with serial, parallel, or hybrid topologies for a given motion pattern [36]. Generally speaking, serial kinematic mechanisms (SKMs) have larger workspace and dexterity, whereas parallel kinematic mechanisms (PKMs) have higher stiffness and payload capacity. Only a small number of multilegged robots use pure serial or parallel topologies. For example, ANYmal [3] and HyQ2Max [15] quadruped robots have pure serial leg mechanisms. PKMs are typically used for the leg structures of high-payload mobile robots [7, 8]. The serial-parallel hybrid mechanism has greater rigidity than the SKM with the same DOF and a larger workspace than the PKM with the same DOF [36]. For some disaster rescue tasks, multilegged robots need both static and dynamic gaits. Furthermore, the actuation and control systems of robotic machines should be protected from potentially harsh environments. A hybrid leg mechanism can be a suitable solution [6]. Table 5 shows the leg configurations of the selected legged robots. Underlining denotes the active joint. The subscripts r , p , and y denote the roll, pitch, and yaw motion characteristics, respectively. \tilde{R} denotes the output joint of the four-linkage mechanism.

There are two main factors that need to be considered for the rigid mechanism design of legged robots: 1) minimizing the leg inertia, and 2) facilitating the protection of the actuation and control systems. For conventional serial manipulators, each actuator is directly mounted on each joint, and thus the inertia of distal links increases greatly. To decrease the leg inertia, the dual coaxial motor design is usually adopted for driving the HFE and KFE joints as shown in Figure 9(a) [37]. Two motors for actuating the HFE and KFE joints are mounted co-axially on the hip joint. The KFE motor actuates the knee joint by a four-bar linkage mechanism. In fact, this kind of leg configuration can be regarded as a five-bar PKM with 2 DOF as shown in Figure 9(b). The key element of this mechanism is

Table 5 Leg configurations of selected legged robots

Name	No. of legs	DOFs of leg	Leg configuration
HyQ2Max [15–19]	4	3	$\underline{R}_r \underline{R}_p (R_p \underline{P} R_p \tilde{R}_p)$
HyQReal	4	3	$\underline{R}_r \underline{R}_p (R_p \underline{P} R_p \tilde{R}_p)$
StarLETH [20]	4	3	$\underline{R}_r \underline{R}_p (R_p \underline{P} R_p \tilde{R}_p)$
ANYmal [10]	4	3	$\underline{R}_r \underline{R}_p \underline{R}_p$
Cheetah 1 [21]	4	2	$\underline{R}_p (R_p \underline{P} R_p \tilde{R}_p) R_p$
Cheetah 2 [22, 24]	4	2	$\underline{R}_p (R_p \underline{P} R_p \tilde{R}_p) R_p$
Cheetah 3 [23, 24]	4	3	$\underline{R}_r \underline{R}_p \underline{R}_p$
Scalf-II [26]	4	4	$(R_r \underline{P} R_r \tilde{R}_r) (R_p \underline{P} R_p \tilde{R}_p) - (R_p \underline{P} R_p \tilde{R}_p) P$
HIT quadruped robot [27]	4	4	$(R_r \underline{P} R_r \tilde{R}_r) (R_p \underline{P} R_p \tilde{R}_p) - (R_p \underline{P} R_p \tilde{R}_p) P$
Baby elephant [28]	4	6	$\underline{R}_r (R_p \underline{P}) S$
CNI robot	4	3	$\underline{R}_r \underline{R}_p \underline{R}_p$
SpotMini	4	3	$\underline{R}_r \underline{R}_p (R_p \underline{P} R_p \tilde{R}_p)$
Laikago	4	3	$\underline{R}_r \underline{R}_p (R_p \underline{P} R_p \tilde{R}_p)$
JueYing	4	3	$\underline{R}_r \underline{R}_p (R_p \underline{P} R_p \tilde{R}_p)$
XDog [29]	4	3	$\underline{R}_r \underline{R}_p \underline{R}_p$
BIT-NAZA	4	6	6 - UPS
Lauron-IV [30, 31]	6	4	$\underline{R}_p \underline{R}_y \underline{R}_r \underline{R}_r \underline{P}$
Crabster [32, 33]	6	4	$\underline{R}_y \underline{R}_r \underline{R}_p \underline{R}_r$
Octopus [34]	6	6	$(UP\&2UPS)S$
Hexbot-IV [6]	6	3	$(RU\&2RUS)$
HIT hexapod robot [35]	6	6	$\underline{R}_y (R_p \underline{P}) S$

a pantograph configuration. From the standpoint of bionics, the pantograph mechanism can mimic the main kinematic features of the mammalian leg, so it is often used in the leg design of walking robots [38]. Furthermore, the pantograph can maintain the relative angular orientation between the proximal and distal leg segments during most of a stride cycle [39]. In addition, the chain drive is also used for the motion transmission from the hip joint to the knee joint. For example, both Cheetah 3 [25] and StarLETH [20] adopt a chain drive for the knee joint. The chain transmission enables the knee joint to rotate along the positive or negative directions as demonstrated in Figure 9(c), thus enlarging the motion range of the knee joint. In order to protect the actuation and control systems, PKMs are usually adopted for concentrating all actuators at the main body. For instance, 18 motors were all placed on the body frame of the Hexabot-IV robot, and the HAA,

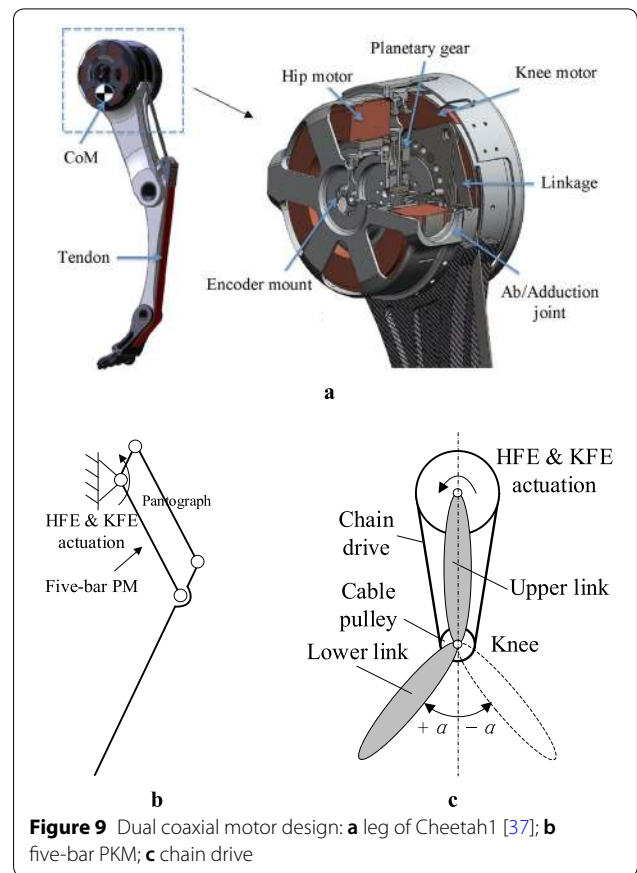
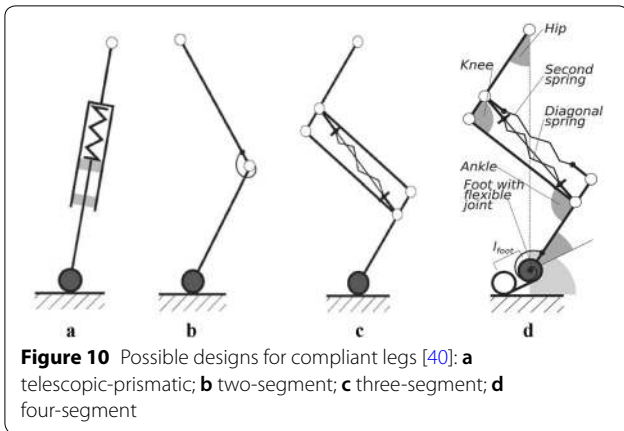


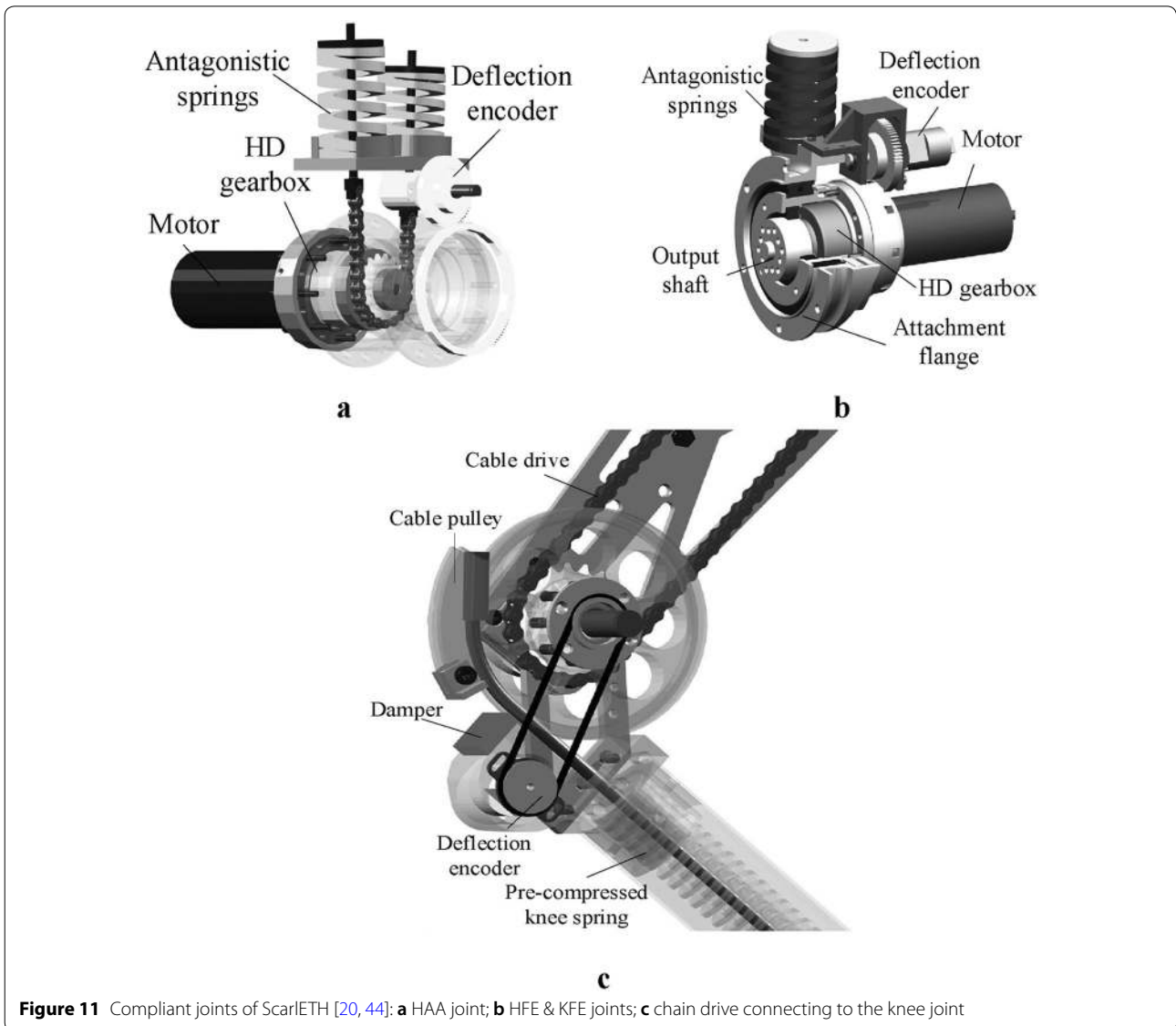
Figure 9 Dual coaxial motor design: **a** leg of Cheetah1 [37]; **b** five-bar PKM; **c** chain drive

HFE, and KFE joints were actuated by a 3-DOF PKM [6], as shown in Figure 8(b).

Recently, more and more compliant mechanisms have been introduced into legged robotics because these flexible systems are perfectly suited to interact with various environments and to handle uncertainties or disturbances such as ground contact collisions. The multisegment leg with compliant elements is an effective biological method to design highly dynamic multilegged robot systems. Leg compliance facilitates long-distance running and improves energy efficiency [40]. There are four possible designs for compliant legs, as seen in Figure 10. The first design is a telescopic/prismatic leg design, such as Raibert’s MIT Quadruped robot [41] and Scout II robot [42]. For instance, each leg of Scout II consists of only an active hip joint and a passive prismatic joint with a damped spring. Using passive dynamics, Scout II can perform bounding and running gaits. Typical examples of the two-segment design are KOLT [43] and StarLETH [20] quadruped robots. The knee joint of KOLT [43] is actuated by a brushless motor and a pneumatic spring, which produce leg flexion and extension, respectively. The pneumatic spring provides the necessary leg compliance at landing and allows elastic energy



to be stored. The StarLETH robot adopts high-compliance series elastic actuators with linear compression springs, as seen in Figure 11 [20, 44]. This mechanism improves the robustness against impacts. Furthermore, by tuning the joint stiffness, the linear compliant mechanism can exploit the natural dynamics of the legged robotic system and therefore the energy consumption can be reduced. The Cheetah-Cub robot adopts the third and fourth configurations [40]. In terms of the third design (Figure 10(c)), there is a diagonal spring spanning the pantograph which provides a leg-extension force at all times. The third design is called the SLP mechanism (spring-loaded pantograph), and the fourth design is called the ASLP mechanism (advanced SLP). Using the ASPL leg design, the Cheetah-cub robot can self-stabilize through



open-loop control. In particular, the Froude number of the Cheetah-cub robot reaches up to 1.3, which means that it was nearly the fastest among all quadruped robots below 30 kg when it was created.

4 Actuation

The highly dynamic legged robotic system puts forward demanding requirements for actuators, such as high robustness against impacts, accurate velocity control, low-impedance force control, and high power density [10]. Dynamic gaits, such as running, require high stride frequency and low duty factor. From the theory of momentum conservation, the relationship between the total vertical impulse F_z and gravity G can be written as

$$\int_0^T F_z dt = GT, \tag{1}$$

where T is the period of cyclic locomotion. From Eq. (1), it is found that the ground reaction force increases with the decrease of the duty factor. In other words, the ground reaction force increases with the increase of speed [45]. The maximum reaction force on each leg is approximately 2.6 times the weight when a dog is running at 9 m/s [46]. To meet the requirement of high output torque, different kinds of actuators with high power density, including hydraulic and electric actuators, have been developed. Among the legged robots listed in Table 4, the

HyQ2Max, HyQReal, and Baby elephant robots adopt hydraulic actuation, and the other robots use electric motors. For dynamic locomotion of legged robots, there are mainly three types of actuation technologies, namely 1) hydraulic actuation for the HyQ series of robots [15–19], 2) quasi-direct drive (QDD) for the Cheetah series of robots [21–24], and 3) serial elastic actuation (SEA) for the StarLETH series of robots [10, 20].

4.1 Hydraulic Actuation

Hydraulic actuators can provide extremely high power density and are naturally robust against impulsive load. Many kinds of legged robots from Boston Dynamics, such as BigDog, LS3, and Atlas, use hydraulic actuators [47], as seen in Figure 12 (left). There are some advantages of hydraulic actuators, like strong robustness to impacts, high power, and great force density. Hydraulic actuators are naturally robust against impacts because impulsive load energy is easily absorbed by hydraulic oil [48]. Hydraulic actuators can provide both high power density and high-level force controllability owing to a high-frequency servo valve with precise pressure sensors [49]. In addition, it is easier to construct high DOF machines using the hydraulic actuation system, which is very important for the future applications of multilegged robots.

Multilegged robots without arms do not have manipulation capabilities. Recently, a quadruped robot with two

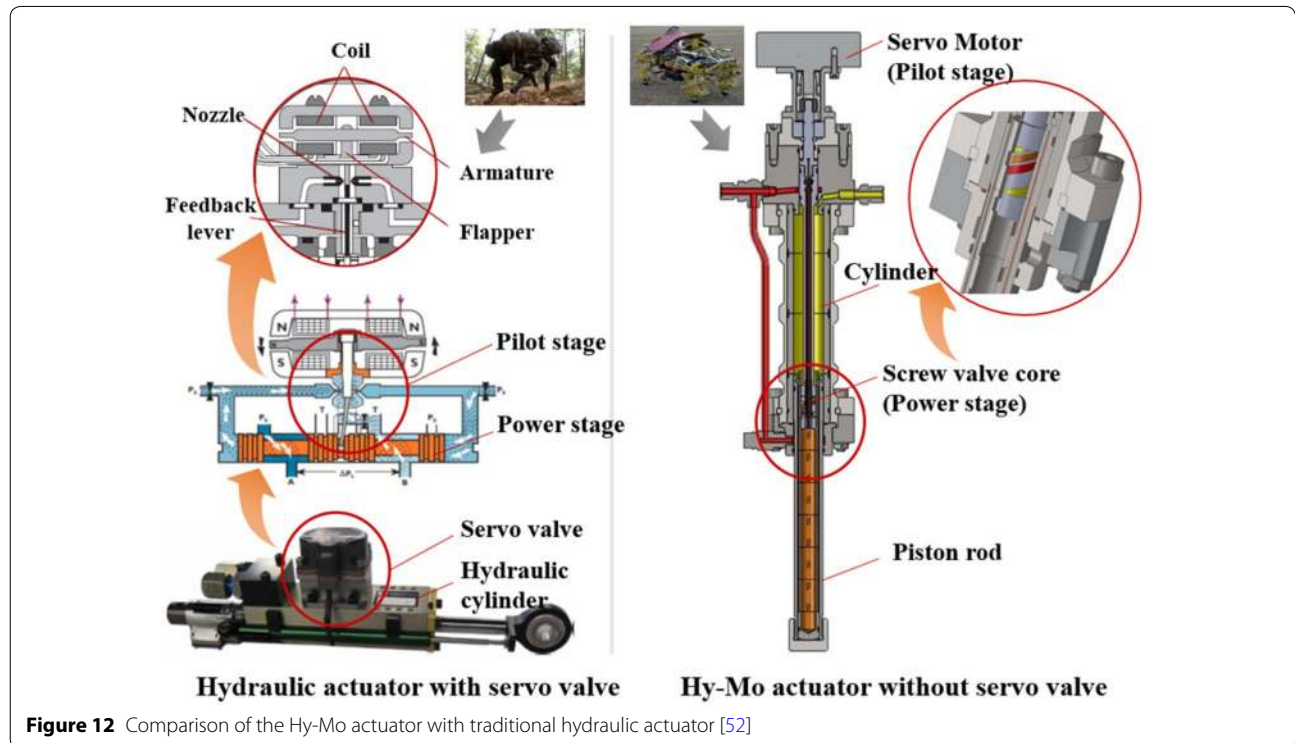


Figure 12 Comparison of the Hy-Mo actuator with traditional hydraulic actuator [52]

6-DOF hydraulically actuated arms, HyQ2Centaur [15, 50], was proposed. The arms have low inertia with high payload capability because most of the hydraulic actuation systems are located in the body frame. For robots actuated by electrical motors, it is very challenging to build a robot system with many DOFs and high-force distal links. However, hydraulic legged robots are usually much larger and heavier than their electric counterparts, which is one of the drawbacks to the scalability of hydraulic actuation systems. Besides, hydraulic actuators also tend to be energetically inefficient because of the fluid viscous loss and internal leakage of the servo valve [51]. The Baby elephant quadruped robot [28] adopts a novel “Hy-Mo” actuator which combines a hydraulic cylinder and servo motor. There is no servo valve for the hydraulic actuation system. A small servo motor with a high-resolution encoder is adopted to control the output position of the cylinder, as seen in Figure 12 [52]. It was found that the leakage of the Hy-Mo hydraulic system is only 10% of the system with a servo valve [28].

4.2 Quasi-direct Drive (QDD)

Thanks to recent advances in electric actuators, the power mass density of servo motors has greatly increased. However, high power is only possible at the range of high speed where the output torque is relatively low. A harmonic reducer with a high reduction ratio is usually adopted to increase the torque density of the servo motor at low speeds. However, the high gear reduction results in the increase of passive impedance, including the reflected inertia, friction, and damping. The joint mechanical impedance is proportional to the square of the reduction ratio [43]. Joints with high reduction ratios do not have back drivability. Without this ability, it is difficult to obtain high bandwidth torque control. The ideal state of joint impedance is that the joint acts approximately as a free joint (without considering the parasitic torque) when it is not actuated by the electric motor [43]. The MIT Cheetah robot introduced a new actuation paradigm (i.e., “proprioceptive electric actuators”) for legged robots. It shows that impressively fast, dynamic legged robots (maximum speed up to 6.4 m/s [22]) can be actuated with electric motors given the right design approach [53]. This actuation strategy has also demonstrated remarkable efficiency, with the COTs of the MIT Cheetah robots being similar to mammalian COTs [21, 24, 54]. The Cheetah series of robots adopts custom-designed high-torque-density (mass-specific torque) electric motors with very low gear reduction to improve the load capacity and low-speed efficiency. For example, the reduction ratios of the planetary gears for Cheetah 2 and 3 are 5.8:1 and 7.67:1, respectively [24]. These actuators with very low reduction ratios are called quasi-direct

drive (QDD) actuators. A QDD actuator can obtain excellent “transparency,” a characteristic which means the reflected inertia of the actuator is much smaller than the output inertia [55]. This is critical for dynamic locomotion. Besides, the torque control based on the current control of the electric motor can be performed at very high bandwidths because the output torque is equivalent to the regulation of the motor current. Thus, each actuator has only one position sensor, no force or torque sensors, and relatively simple transmission.

For QDD actuators, the development of high torque density motors is very important. There are two key evaluation indices for electric motors, i.e., peak specific torque K_{ps} for instantaneous performance and thermal specific torque K_{ts} for steady performance [56], which are denoted by

$$K_{ps} = \frac{K_t i_p}{m}, \quad (2)$$

$$K_{ts} = \frac{K_t}{m} \sqrt{\frac{1}{R_{th} R}}, \quad (3)$$

where K_t , i_p , m , R_{th} , and R denote the torque constant, peak current, motor’s mass, thermal resistance, and electrical resistance. These two measures are directly related to the gap radius of the motor [57]. Figure 13 shows the change of K_{ps} and K_{ts} with respect to the gap radius for some motors commonly used in legged robots. Although QDD actuators have been successfully used for small legged robots such as the Cheetah robots, the proprioceptive electric actuator with low gear reduction ratio cannot meet the actuation requirements of large-scale legged robots.

4.3 Serial Elastic Actuation (SEA)

To compensate for the low torque output of the direct drive system, high gear reduction is often used to produce the low speed/high torque characteristics desirable in most legged robot applications. However, gear reduction yields significant friction and reflected inertia at the output shaft, and thus the actuator’s impedance becomes extremely large. By adding series elasticity to these conventional systems as in Figure 14(a), we can attain a force-controllable actuator with low impedance, low friction, and good bandwidth and thus achieve high-quality force control [58]. By measuring the compliant element’s deflection, the output torque can be calculated using Hooke’s Law. Accordingly, the output torque can be controlled by spring deflection. In the meantime, the elastic element can store energy and increase peak power while the spring and servo motor do work in the same

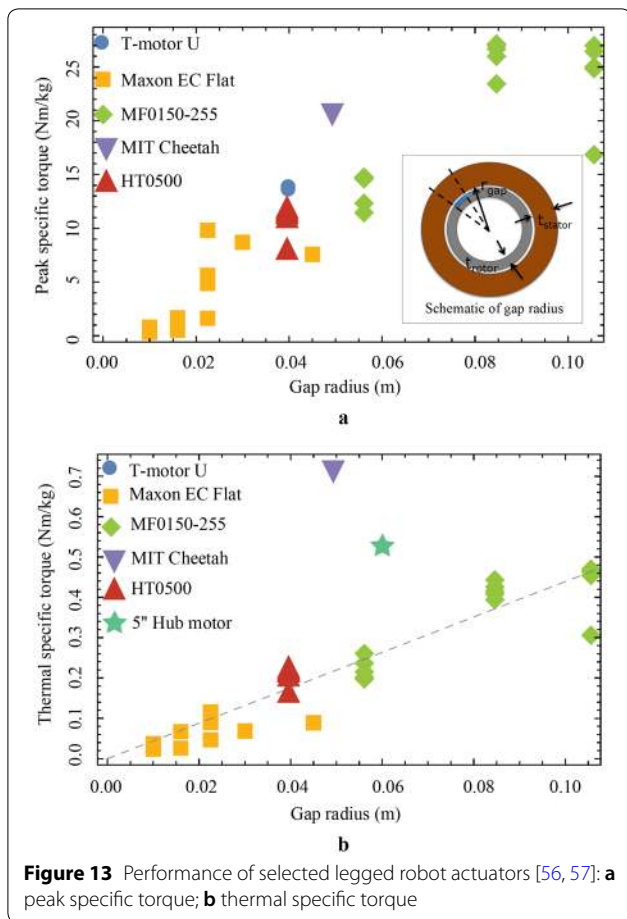


Figure 13 Performance of selected legged robot actuators [56, 57]: **a** peak specific torque; **b** thermal specific torque

direction. Besides, the compliant element can protect the gearbox from being damaged during impact.

The implementation of SEA turns the torque control into a position control case. Figure 14(b) shows a typical SEA control architecture [10], which is a cascade controller including the inner torque and outer position control loops. There is a PID controller, friction compensation, and a feed-forward term for the torque control loop. In Figure 14(b), τ^{des} , θ_j , θ_g , and k denote the desired torque, joint position, gear position, and the SEA stiffness coefficient. There are usually two position sensors for measuring θ_j and θ_g . Therefore, the real output torque τ can be computed according to the k value and the spring deflection (i.e., the difference between θ_j and θ_g). However, the SEA actuators have some detriments owing to the substantial delay and limited bandwidth in the position control, especially when legged robots run at high speeds. Quadruped robots actuated by SEA actuators do not have the actuation performance necessary to execute the sorts of dynamic maneuvers like high-speed running which have been demonstrated on the MIT Cheetah robots and the hydraulic robots from Boston Dynamics [53].

5 Perception

5.1 Sensors

There are two groups of commonly used sensors, namely proprioceptive sensors for measuring the states of each joint and the robot body and exteroceptive sensors for measuring environmental information, as seen in Figure 15. The former group includes encoders, inertial measurement units (IMUs), and torque sensors. The environmental information measured by the latter group consists of geometrical parameters such as the outline dimensions of an obstacle, the slope of the ground, and physical parameters, such as contact force, temperature, humidity. To measure these geometrical parameters, both visual and non-visual sensors are adopted. Common visual sensors include binocular cameras and RGB-D (red-green-blue-depth) cameras. Binocular vision usually employs two CCD (charge-coupled device) or CMOS (complementary metal oxide semiconductor) sensors to perceive a single three-dimensional image of its surroundings. RGB-D cameras (such as Intel Realsense) can capture visual RGB images along with per-pixel depth information, which can be transformed into the coordinates of point clouds. RGB cameras rely on either active stereo or time-of-flight sensing to estimate the depths of a large number of pixels. However, RGB-D cameras can provide sensing for a limited distance (less than 5 m), and the depth estimation is noisy (typically about 3 cm at 3 m depth) [59]. Besides, vision sensor data are easily contaminated by

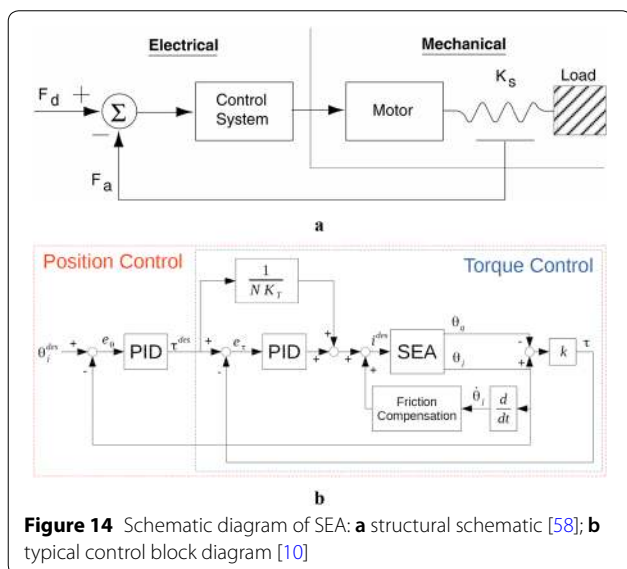
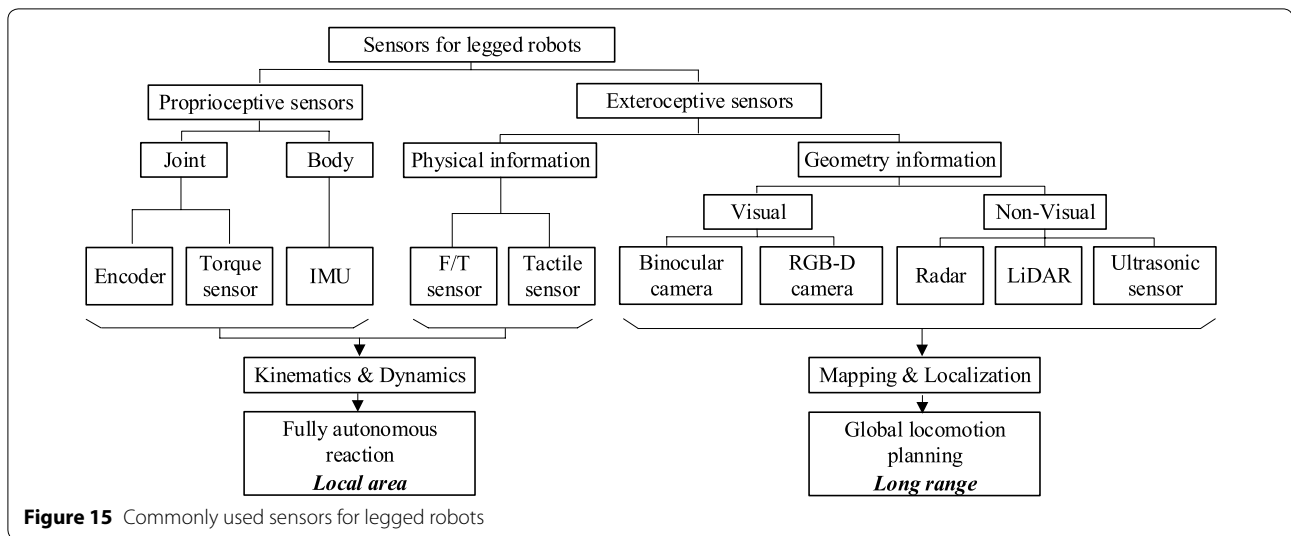


Figure 14 Schematic diagram of SEA: **a** structural schematic [58]; **b** typical control block diagram [10]



illumination. Thus, RGB-D cameras are mainly suitable for indoor dense 3D modeling. Non-visual sensors usually obtain a 3D point cloud by measuring distances, such as in the cases of radar, LiDAR (light detection and ranging), and ultrasonic sensors, the measuring precision of which is higher than visual sensors [14]. In addition, to sense environmental physical parameters, such as contact force, a multi-axis force and torque sensor is often mounted on the body or at the end of the leg since force perception is very important to the dynamic control of legged robots.

Multisensor fusion is an important trend for intelligent legged robots. For instance, the BigDog robot includes a number of different sensors, such as IMU, 3D camera, odometer, and GPS to perform state estimation [60]. Each sensor has its advantages and its share of disadvantages, such as LiDAR's failure in rain, the short range of the ultrasonic sensor, and the low angular resolution of radar, which makes it necessary to employ a suite of sensors when designing navigation systems to overcome the limitations of each sensor alone [61]. For example, on uneven terrain, geometrical information (such as a 3D point cloud) from visual or non-visual sensors is contaminated by system vibration and the rotation and translation of the legged robot body. The pose noise must be eliminated through robot pose compensation. The IMU sensor is usually mounted on the legged robot to estimate the legged robot's pose. The IMU sensor consists of 3-axis gyro sensors and 3-axis acceleration sensors, and thus the estimated output state is 6-DOF angular velocity and acceleration. Visual perception fused with IMU sensing is very important to guarantee the stable operation of a legged robot [62].

5.2 Mapping

The autonomous locomotion of legged robots is a complicated task ranging from low-level motor control to high-level cognitive processing [63]. The autonomous ability of the legged robot is related to the global locomotion planning in the long range and the fully autonomous reaction in the local area. In this paper, "long range" is defined as an activity that takes the legged robot beyond the horizon of the robot's environment sensors, and the "local area" is the scope within a gait period. The former mainly depends on the perception of geometrical parameters, whereas the latter (to be further discussed in Section 6) depends on kinematic and dynamic modeling and the perception of physical parameters, as seen in Figure 15. The state of the art regarding the mapping and localization of legged robots is presented below and in the following subsection.

The locomotion performance of a legged robot heavily depends on mapping for navigation and planning. Point cloud data are obtained by stereo vision [64] or laser sensor [62]. The raw data of 3D point clouds cannot be used directly for mapping because they require a large amount of memory. Thus, point clouds must be changed into a grid map, which means that the world is divided into a regular, two-dimensional grid of evenly spaced cells. Gutmann et al. [65] presented a grid map including the height information of the floor covering the cell area. Rekleitis et al. [66] proposed irregular triangular meshes (ITMs) to represent the environment. ITMs inherently support concave geological structures like overhangs and caverns, unlike digital elevation maps (DEMs). Ishigami et al. [67] presented an elevation map with cylindrical coordinated terms, called C^2 DEM, which achieves range-dependent resolution for terrain mapping and generates

a detailed terrain representation near the robot. Khan et al. [68] proposed a rectangular cuboid approximation framework (RMAP) using axis-aligned rectangular cuboids (RC), which is able to generate probabilistic 3D representations with multiresolution capabilities.

Compared to wheeled or tracked robots, legged robots are better able to traverse obstacles in harsh environments. Legged robots have more choices, such as stepping on, stepping over, or bypassing obstacles. Thus, the map for the legged robot's locomotion must contain explicit geometric features of the partial terrain. However, few works involve this process. Recently, Chai and Gao [69] presented a novel geometric feature grid map (GFGM) to describe the terrain for legged robots, which is useful for checking obstacles and finding paths in cluttered environments.

5.3 Localization

Localization is another key capability for autonomous legged robots and is typically performed using a combination of odometry (from joint encoders or visual sensors) and inertial sensing (from IMUs) [60]. When legged robots work in an unexplored environment, simultaneous localization and mapping (SLAM) is an important technique. SLAM is a solution that allows a mobile robot to incrementally build a consistent map of an unknown environment while simultaneously obtaining the location of the robot within this map [70]. Either a camera or a laser can be used as the primary sensor for the implementation of SLAM, with the corresponding methods called Visual-SLAM and LiDAR-SLAM, respectively. There are two main computational solutions to the SLAM problem, i.e., the extended Kalman filter (EKF-SLAM) [71] and Rao-Blackwellized particle filters (Fast-SLAM) [72]. Presently, computational complexity, data association, and environment representation are three main research areas in the development of SLAM. Many algorithms relevant to these research areas have already been developed, such as UKF-SLAM [73], Graph-SLAM [74], Mono-SLAM [75], and Co-SLAM [76]. Although SLAM has reached a state of considerable maturity, it is still a great challenge to generate consistent maps of large areas [14]. However, legged robots frequently enlist SLAM to deal with large unstructured areas such as planetary surfaces and disaster scenarios [77].

Multisensor data fusion algorithms considering legged robots' characteristics may be available for the solution of large-scale SLAM problems. The HyQ robot can perform goal-oriented navigation within unknown harsh terrain using IMUs and RGB-D vision [63]. A novel multisensory data fusion algorithm has been exploited for the DLR Crawler hexapod robot, which fuses measurements from an IMU, 3D visual odometer, and 3D leg odometer

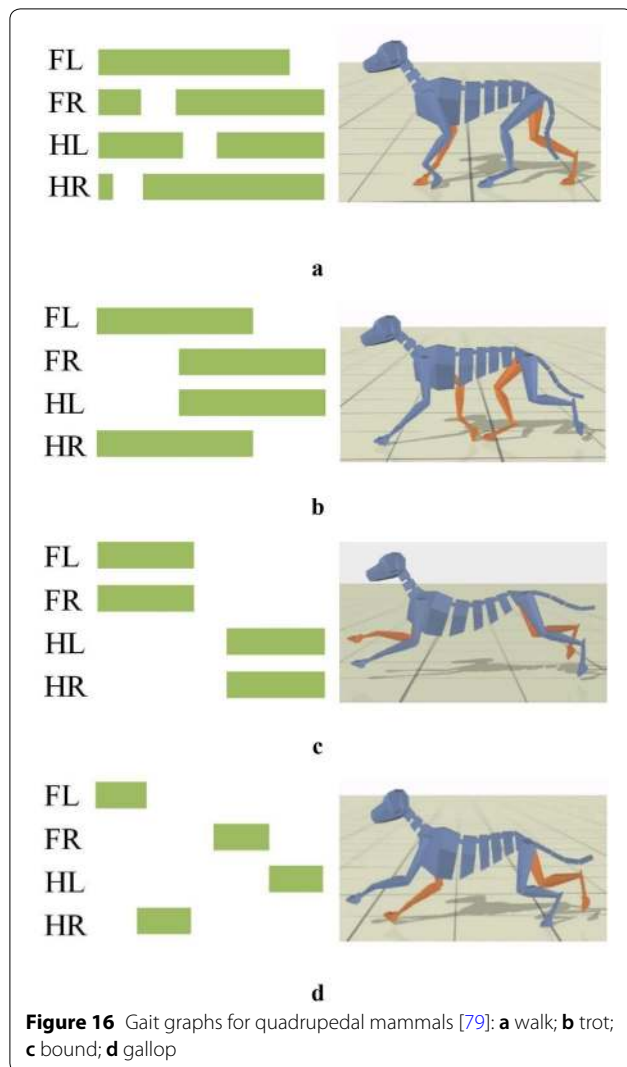
[64]. The leg odometry measurements enable the robot to sense areas with low visibility, such as shadowy areas. Compared to using only a single sensor, multisensor fusion algorithms improve both robustness and pose estimation accuracy. However, the error model for the leg odometer needs to be further developed to automatically adjust the weights of incorrect odometry measurements in the fusion process.

6 Control

6.1 Gait Patterns

The gait is a manner of walking or running on foot. There are three technical terms to describe the gaits of legged robots, namely stride, duty factor, and relative phase [78]. The stride is the distance of leg movement during one cycle. The duty factor of one leg is the ratio of the stance duration to the whole period. Compared to an arbitrarily chosen reference leg, there is a delay before setting down another leg. The relative phase of one leg is defined as the ratio of the delay to the whole period. The gait can be classified as walking or running. The duty factors of walking gaits are generally greater than 0.5, whereas those of running gaits are generally less than 0.5. For example, trotting, cantering, and galloping are all running gaits. There are also symmetric and asymmetric gaits, which are usually used by quadrupedal mammals for slow and fast running, respectively. For instance, the trot and the gallop are the most common running gaits used by quadrupedal mammals. The symmetric trot gait is predominant in low and moderate speeds, whereas the asymmetric gallop gait is preferred in higher speed running. Figure 16 shows common gait graphs for quadruped robots [79]. The stance phases are drawn as green bars whilst the swing phases are drawn as empty bars. For hexapod robots, there are usually three kinds of gaits, namely alternating tripod, wave, and free gaits [80]. The alternating tripod gait, whose duty factor is about 0.5, is typically selected for high speed walking on relatively flat terrain. The wave gait is more suitable for lower speed walking on difficult terrain, and its duty factor is more than 0.7.

Despite the diversity in morphology, mammals of different sizes have similar gait characteristics, i.e., dynamic similarity, which gives important inspiration for the design of legged robots. First, they tend to adopt the same gait while moving with equal Froude numbers [78]. The Froude number is written as $F_r = v^2/gL$. Here, v , g , and L are the velocity, gravitational acceleration, and the height of the hip joint at standing. The Froude number has widespread applications in the biomechanics of legged locomotion [81]. For example, quadrupedal mammals usually change gait from trotting to galloping at a Froude number of 2–3 [78]. Second, though quadruped mammals and hexapod insects have different amounts of



legs, there are similar ground contact behaviors for two legs in quadruped mammals and three legs in insects, just like one leg in human beings [82]. The whole-body mechanics in two-, four-, and six-legged runners can be remarkably similar, despite variations in body form or morphology [83]. This characteristic enables the leg design and control of both quadruped and hexapod robots to be implemented using the same method such as the spring-loaded inverted pendulum (SLIP) model [84]. For those gaits that use the support legs one at a time, such as trotting with diagonal pairs, pacing with lateral pairs, and bounding with front and rear pairs, one-leg algorithms can be used to control quadruped robots [85] and hexapod robots [86].

6.2 Gait Control

Control and motion planning of legged robots faces several challenges, such as high-dimensional systems with

floating base and redundant DOFs and whole-body multi-contact interactions with unknown environments [87]. Here, motion planning refers to the aforementioned local area within a gait period. To lower control complexity, dynamic locomotion is usually decomposed into several simpler tasks such as body stabilization, leg motion planning, and ground reaction force control. Many methods have been developed for gait control, which can be grouped into three categories, namely kinetostatics-based methods, dynamics-based methods, and model-free methods.

Kinetostatics-based control methods are mainly exploited for static gaits to provide center-of-gravity (COG) projection [88] and find the zero moment point (ZMP) [89]. The ZMP is an extension of the COG method including the inertia force, and it is a point on the ground where the resultant moment of the multi-legged robot is zero. When the ZMP is located within the supporting polygon, the legged robot is stable. The ZMP criterion is effective for controlling the low-speed walking of quadruped [90] and hexapod [91] robots. To further evaluate the stability degree, the ESM (energy stability margin) [92], CSSM (compliant static stability margin) [93], F-ASM (force-angle stability margin) [94], and DSM (dynamic stable margin) [95] were proposed for the gait control of legged robots. However, these kinetostatics-based approaches are not suitable for running gaits, such as trotting and galloping. This is because there is no obvious polygon for the ZMP calculation when legged robots are running with high speed. Furthermore, from the energy consumption perspective, the ZMP control method is not economical because the legged robot's torso with a large mass has to be accelerated and decelerated in each gait stride.

Compared to kinetostatics-based control, the latter two methods are more suitable for the high-speed control of legged robots. This paper focuses on the control of highly dynamic locomotion. The present statuses of dynamics-based and model-free control methods will be surveyed in Sections 6.2.1 and 6.2.2. These two kinds of control methods have been widely used for highly dynamic legged robots, as seen in Table 6. Dynamics-based control methods include the SLIP model [6, 43, 47, 56, 85, 96, 97], virtual model control (VMC) [98, 99], model predictive control (MPC) [24, 100, 101], whole-body control (WBC) [3, 10, 20, 87, 102–104], and so on. Model-free methods include the commonly used central pattern generator (CPG) control [17, 40, 105–108], sim-to-real reinforcement learning (RL) [3, 109, 110], and so on. A CPG can utilize a legged robot's inertia to minimize energy consumption and simultaneously allow for free-gaits that are robust to disturbances. The CPG-based control method has also been adopted to generate dynamic gaits [40, 105,

Table 6 Dynamic gaits and control methods of selected legged robots

Categories	Robots	Mass (kg)	v_{\max} (m/s)	F_r	Gaits	Control methods
Dynamics-based control	Quadruped [85]	38	2.2	0.88	Trot	SLIP
			2.9	1.53	Bound	SLIP
	Minitaur [56, 96]	5	0.8	0.374	Pronk	SLIP
			1.45	1.23	Bound	SLIP
	SCOUT II [97]	20.865	1.3	0.53	Bound	SLIP
	BigDog [47]	109	3.1	0.98	Bound	–
			2	0.41	Trot	–
	KOLT [43]	80	1.1	0.18	Trot	SLIP + Fuzzy Control
	Hexbot-IV [6]	268	0.55	0.04	Trot	SLIP for hexapod tripod gait
	HyQ [99]	70	1	0.15	Trot	VMC
	HyQ [48, 162]	70	2	0.6	Trot	Active impedance control
	Cheetah 1 [112–114]	39.406	6	7.34	Gallop	Proprioceptive impedance control
	Cheetah 2 [2, 22, 54]	34.4*	6.4	7.1	Bound	Direct control of ground reaction force
	Cheetah 2 [1]	34.4*	2.4	1	Jump over obstacles	MPC
	Cheetah 3 [24, 100, 101]	45	1.2	0.216	Trot	MPC
			1.7	0.434	Flying-trot	MPC
3			1.35	Gallop	MPC	
StarLETH [20, 102–104]	25	0.7	0.15	Trot	WBC	
ANYmal [10, 87]	30	1	0.204	Trot	WBC	
Model-free control	Cheetah-cub [40]	1.1	1.42	1.3	Trot	CPG
	Tekken 1 [40, 105, 106]	3.1	1	0.49	Trot	CPG
			1.1	0.59	Bound	CPG
	Tekken 2 [40, 107]	4.3	0.95	0.37	Trot	CPG
	HyQ [17]	70	0.35	0.104	Trot (On unexpected terrains)	CPG-Task space trajectory generation
	Baby elephant [108]	130	0.5	0.035	Trot	CPG
	Minitaur [110]	5	0.6	0.21	Trot	Sim-to-real RL
		1.18	0.815	Gallop	Sim-to-real RL	
ANYmal [3]	30	1.5	0.459	Flying-trot	Sim-to-real RL	

* The mass is estimated from the data in Refs. [1] and [22]

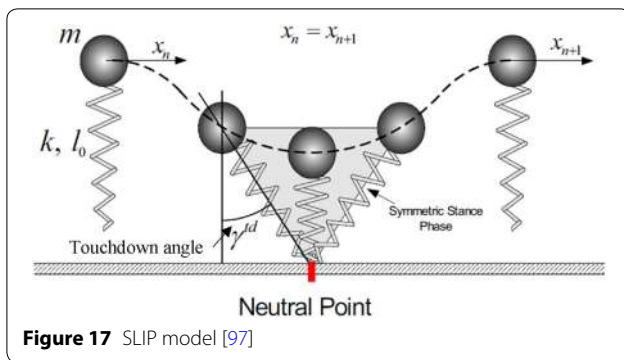
107]. Sim-to-real RL [3, 110] has recently been exploited for the control of multilegged robots. For example, using this compelling method, the ANYmal quadruped robot achieved dynamic locomotion performances that could not be obtained by conventional control approaches [3].

6.2.1 Dynamics-based Control

An important distinction between static and dynamic gaits is the stability criterion. For dynamic gaits, the static stability criterion such as ZMP is no longer suitable for the state estimation of legged robots. Based on a fast feedback loop, a legged robot obtains dynamic stability by continuously moving the feet or the body. Gaits can be regarded as the byproduct of preserving the stability of the legged robot [111]. The dynamic stability criteria of legged robots are still in question. Because the locomotion of a legged robot is typical periodic motion, Poincaré return map analysis has been widely adopted to evaluate

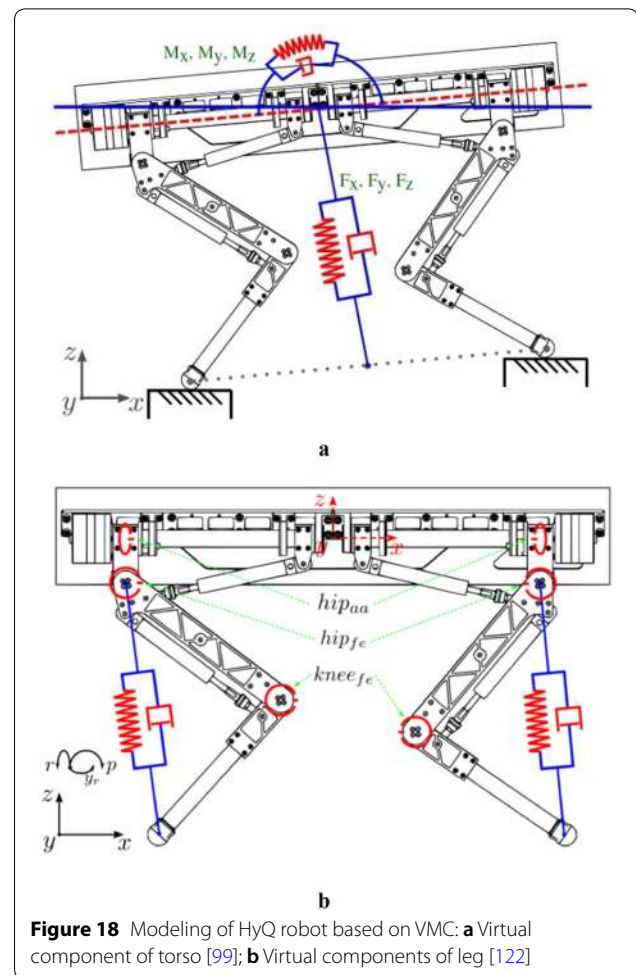
locomotion stability [22, 112–114], from the relatively simple SLIP control model [97] to more complicated models involving specific configuration such as hybrid leg mechanisms [6].

SLIP model. Animals have very distinct force and motion patterns when they are running. During walking, the potential and kinetic energies of the torso change in either a sinusoidal or out-of-phase manner. Therefore, the changes of kinetic and potential energies can be described by a pendulum-like energy recovery mechanism. Cavagna et al. [115] first proposed the SLIP model to mimic the dynamic characteristics of a variety of animals. SLIP is represented by a point mass atop a spring as shown in Figure 17 [97], which is passive and conservative. A stride in the SLIP model consists of the stance and flight phases. The body tracks a ballistic trajectory under the influence of gravity, and the springy leg adjusts the touchdown angle to swing



to the desired position in the flight phase. The mass moves forward in the stance phase by compressing and decompressing the spring. Raibert et al. [84, 85] presented three servo loops that controlled the running speed, body attitude, and hopping height. Although the controller is very simple, legged robots can obtain robust dynamic gaits with high performance, such as the trot [6, 43, 85], pronk [56, 96], and bound [85, 97]. Despite morphological and design differences, most of these robots adopted the SLIP control method without intense feedback [97]. Furthermore, if the SLIP model is provided with suitable initial conditions, including touchdown angle, the legged robot can tolerate small disturbances without feedback control [116]. However, the control precision of SLIP needs moderate improvement, especially in tracking the desired velocity. The fuzzy controller can learn the leg touchdown angles and leg thrusts in one stride [117], and thus it has been adopted to improve the velocity and height tracking characteristics for legged locomotion [43].

Virtual model control (VMC). VMC, presented by Pratt et al. [98], is an intuitive control scheme for legged locomotion. Compared to SLIP, which highly depends on tuning or optimization, the VMC has a virtual model to generate the desired actuator torques. The VMC puts virtual elements between contact points, such as the spring, damper, dashpot, mass, latch, bearing, and non-linear potential and dissipative field. There are three obvious merits of the VMC. First, complex tasks can be easily described using simple virtual components. For instance, the HyQ uses the virtual model approach to enact robot stabilization control. Two virtual spring-damper components between the torso and the contact surface are used for VMC modeling, as shown in Figure 18 [99]. The virtual forces and moments are calculated and then transformed to feedforward torques for the joint actuation of supporting legs. Second, the VMC needs relatively small amounts of computation.



Third, the VMC can be readily extended to perform complex control tasks by using adaptive and learning elements [118, 119], stiffness control [120], and active impedance control [121, 122]. Recently, Gehring et al. [123] established mappings from virtual forces and torques on the torso to virtual leg forces and then to joint torques. They used this technique to realize the control of the whole body of the StarLETH robot. Furthermore, Xie et al. [124] presented a whole-body VMC method for quadruped robot trotting with special attention to rotation along the body's diagonal line.

Model predictive control (MPC). MPC can be used to solve mode-based optimization problems iteratively by both considering the system's current state and anticipating its future evolution [125]. When the timespan between two hybrid events (such as touchdown or lift-off) is considered, MPC can be used to optimize states and control inputs for a finite horizon with some linear constraints and thus generate stable motions [126]. Typically, the objective function [127] at step i is

$$V(\mathbf{x}_i, i) = \Phi(\mathbf{x}_N) + \sum_{j=i}^{N-1} r(\mathbf{x}_j, \mathbf{u}_j, j), \quad (4)$$

where \mathbf{x}_i denotes the system state, \mathbf{u}_i denotes the control policy at step i , $\Phi(\mathbf{x}_N)$ is the terminal cost, and $r(\mathbf{x}_j, \mathbf{u}_j, j)$ is the cost function. Given a nominal step period, the state evolves as

$$\mathbf{x}_{i+1} = \Phi(\mathbf{x}_N) + \sum_{j=i}^{N-1} r(\mathbf{x}_j, \mathbf{u}_j, j). \quad (5)$$

At each time step, the optimization generates the best \mathbf{u}_i being applied to the legged robot system. Conventionally, the MPC problem can be formulated as a quadratic programming (QP) problem. Though MPC has been widely adopted for ZMP optimization and footstep planning for humanoids [128], MPC is seldom exploited for the gait planning of multilegged robots [1]. Recently, the computational expense of online MPC methods has been greatly decreased by using interior-point [129] and active-set [130] solvers. Furthermore, thanks to recent advancements in convex optimization [131] and its applications to MPC [132], open-source solvers, such as ECOS [133] and qpOASES [134] can solve MPC problems rapidly and reliably. The MPC problem of Cheetah 2 can be computed in 250 μ s by the qpOASES solver, which realizes online planning for autonomous running jumps over obstacles with the speed of 2.4 m/s [1]. Carlo et al. [100] found that an accurate instantaneous dynamic model is more important than a highly accurate model of a legged robot's dynamics during the prediction horizon. Therefore, the dynamic control of a multilegged robotic system based on the MPC method can be formulated as a convex optimization. For instance, Cheetah 3 [24, 101] employs convex MPC to control the ground reaction forces and achieves high robustness of dynamic locomotion at a variety of speeds.

Whole-body control (WBC). The whole-body framework developed by Khatib et al. [135, 136] is a very appealing control architecture for complex tasks with priorities between tasks. Although the implementation that produces control signals of all active joints may be a WBC problem [87], most studies approach WBC problems by considering the floating base inverse dynamics [137]. The dynamic locomotion control of high-dimensional multilegged robots usually decouples motion planning from motion control [138, 139]. The WBC facilitates such decoupling because it is easy to fulfill multiple tasks while simultaneously respecting the behaviors of the legged robot. Farshidian et al. [140] proposed a task space decomposition method that eliminates the coupling between contact force and non-contact controllers. The

WBC formulates locomotion control as an optimization problem considering the full dynamics of the legged robot, and then all joints' desired motion tasks can be achieved. However, solving the optimization problem in real-time is still a great challenge because the computational requirements are very high. To address this challenge, the dynamics and constraints of the legged robot can be formulated as linear constraints with convex cost functions, such as a QP [141]. The combination of searching for solutions in the null space of higher priority tasks and handling explicit inequality constraint problems yields a relatively small QP problem as equality constraints are involved in the cascade of QPs [142]. Thus, the WBC coupled with hierarchical optimization (HO) can be implemented in a legged robot with a real-time control loop at the 1 kHz level. Recently, StarLETH [20, 102–104] and ANYmal [10, 87], two fully torque-controllable quadruped robots, achieved impressive locomotion performance using the WBC method. The robots can traverse unperceived obstacles without the requirement of motion planning from the operator.

Compared to SLIP, VMC, and MPC, WBC has three advantages by incorporating the full dynamics of the legged robot. First, it is capable of dealing with almost all constraints, which is more difficult with the other methods [140, 142]. Second, there are no explicit trajectories to be tracked at the joint level, which increases the compliance of legged robots and decreases the complexity of motion planning [20, 87]. Third, WBC realizes upper-level control more easily because it provides an abstract formulation for the planning [10, 102–104].

6.2.2 Model-free Control

It is clear that the above model-based methods have obtained impressive control performance in multilegged robots. However, there are still two main disadvantages: (i) the limited detail used in the modeling inevitably yields compromises in performance such as agility, compliance, and energy efficiency; (ii) the development of model-based controllers is extremely labor-intensive. In model-free approaches, there is neither a kinematic nor a dynamic model of the legged robot involved in the control. An early model-free control method was the CPG method. Recently, some learning models have been incorporated in optimized controllers [3, 143]. Thanks to the intrinsic simplicity of model-free methods, model-free control is an appealing method for the dynamic locomotion control of multilegged robots.

Central pattern generator (CPG). It is universally known that animal walking is primarily generated by a combination of a CPG and reflexes [105]. The CPG consists of layers of neuron pools coupled with oscillators in the spinal cord, whose outputs are converted into

rhythmic control signals that drive the leg extensor and flexor muscles [144]. The spinal reflexes are in charge of the selection of gait patterns, the timing of swing and stance activities, and the adjustment of CPG outputs [107]. In robot control, the “reflex” refers to the joint torque generation resulting from the sensor information and the response as CPG phase adjustment based on the sensory feedback to the CPG [105]. The CPG controller can not only produce well-coordinated leg movements but also accomplish gait transitions with simple descending control signals [145]. Moreover, the controller can use a neural oscillator (NO) with reinforcement learning to obtain parameters online [146] and optimize various parameters [147]. A great deal of previous research regarding the CPG model attempted to generate dynamic locomotion, such as in the Tekken 1 and 2 [105–107], Cheetah-cub [40], HyQ [17], and Baby elephant [108]. Recently, the design team of Tekken robots used a leg loading feedback mechanism to each CPG for the posture control of a new quadruped model instead of vestibular feedback, as seen in Figure 19 [148]. Using the proposed CPG model with leg loading feedback, robot gaits can autonomously transition from walking to trotting and then to transverse galloping along with its acceleration or deceleration, similarly to animals. Furthermore, interlimb coordination during gait transitions can be self-organized using the CPG model with physical communication throughout the body [143].

There are two obvious trends for CPG control: (i) the external sensory information, such as the robot torso’s postures [105], touchdown feedback [107], and leg loading [148], is applied to the CPG model to improve control performance; (ii) the CPG is combined with another control method, such as inverse dynamics [17, 108], RL [143, 146, 147], or VMC [149]. There are also some issues that need to be further studied. For example, CPG with feedback is likely to degrade the compliance of legged robots, and the situation will get worse if position control is adopted [127]. Nevertheless, CPGs provide an impressive approach to generate gait trajectories by using the limit cycle behavior of coupled NOs to produce joint control signals in real time [150]. CPG-based control greatly reduces the control dimensionality of legged robots while remaining highly flexible to gait patterns.

Sim-to-real reinforcement learning (RL). RL has obtained tremendous progress in recent years, and many algorithms have been developed to cope with autonomous locomotion problems [151–153]. These are data-driven methods, which promise to avoid the aforementioned limitations of model-based approaches. However, there are two difficulties in applying RL to locomotion control. First, RL typically requires weeks or months of training to generate highly agile and efficient algorithms [154]. Second, learning methods cannot be directly applied to physical prototypes because of the possibility of sudden and chaotic behaviors during training [152]. Simulations are appealing environments because

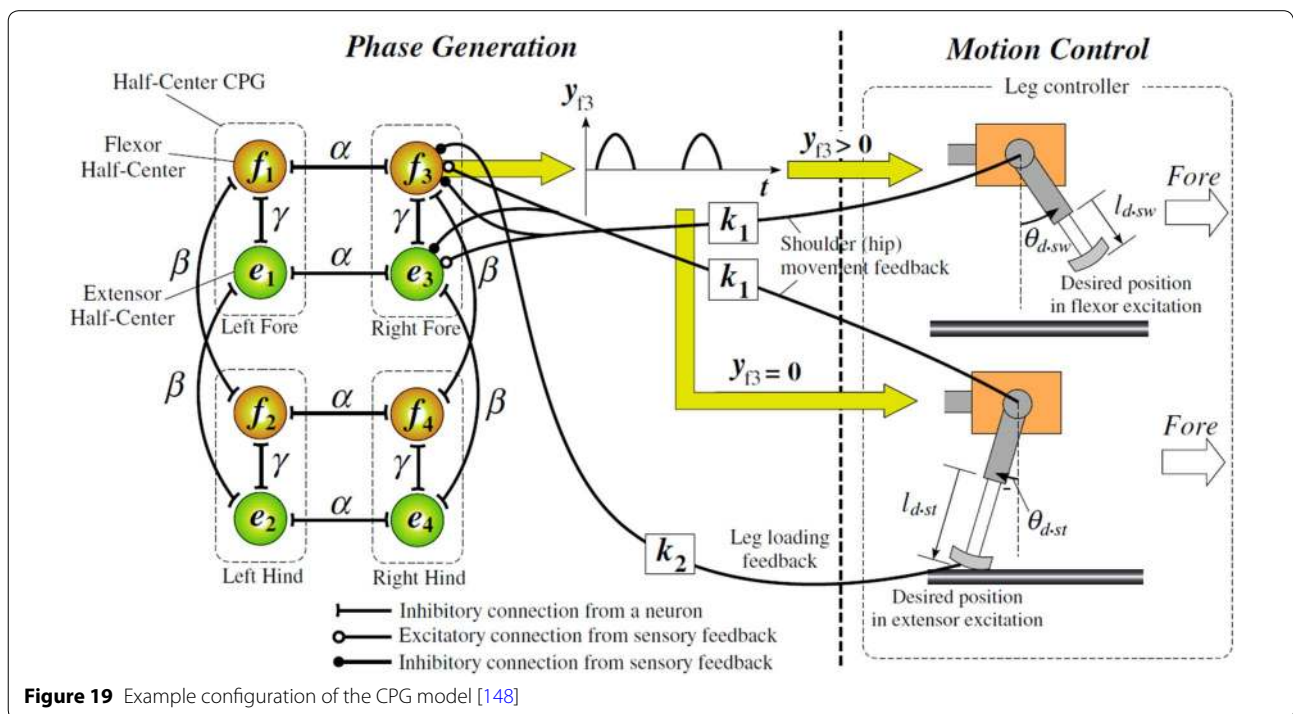
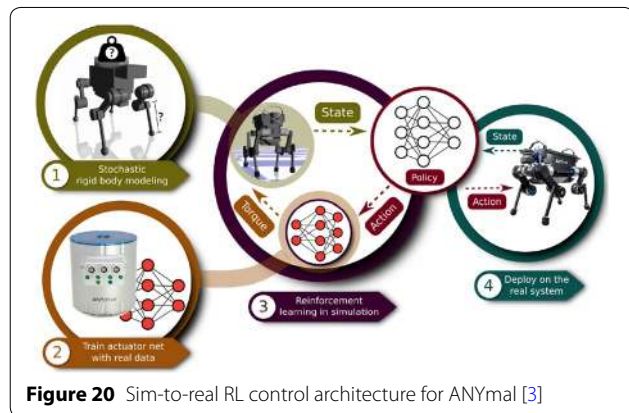


Figure 19 Example configuration of the CPG model [148]

they can provide abundant data for machine learning. Unfortunately, there exists a “reality gap” [155] between real and simulated systems because of such factors as unconsidered dynamics, incorrect model parameters, and calculation errors [109]. The reality gap can be eliminated by improving the simulation fidelity or the robustness of the controller to variations. Lee and Park [156] improved the simulation accuracy of a high-DOF legged robot by inertial parameter identification. The robustness can be obtained by a large amount of training that involves numerous randomization aspects. For example, Xue et al. [110] used dynamic randomization to develop effective policies that can be transferred directly to the real world. Tan et al. [109] achieved a robust controller by adding perturbations in a compact observation space and randomizing the physical environments. After learning in simulation, a quadruped robot called Minitaurs can successfully implement dynamic gaits of trotting and galloping in the real world. This method depends on the analytical actuation model, which can be easily obtained for the direct-drive actuator used in Minitaurs. However, it is very difficult to obtain for complex actuators, such as SEA and hydraulic actuators. Recently, Hwangbo et al. [3] proposed an effective learning approach to deal with a high-performance locomotion controller with SEA actuators. This approach was successfully used for the ANYmal quadruped robot. First, the physical parameters of the robot were identified, and the uncertainties were estimated. Second, an actuator net with complex actuator dynamics was trained. Third, based on the models generated in the first two steps, the control policy was trained. Finally, the trained policy was deployed directly on the physical system, as seen in Figure 20.

6.3 Energy Efficiency

Energy efficiency is one of the most important parameters to be minimized in the control of dynamic locomotion. The energy efficiency is related to the gait pattern,

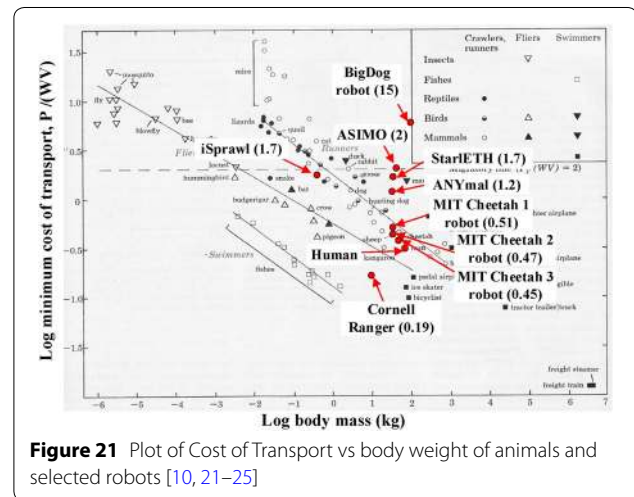


stride, and duty factor. Biological research on animals shows that there exists an optimal speed for each kind of gait pattern which leads to the lowest energy consumption [157]. To achieve the optimal energy-saving mechanism, animals usually select walking gaits at low Froude numbers and running gaits at high Froude numbers [158]. Furthermore, there exist resonant frequencies at which the locomotion energy consumption is minimal. Animals can keep their energy consumption at minimum by tuning their body resonance when they change their speeds [159]. Hoyt et al. [160] proposed a set of relationships between the mechanics, gait parameters, and energetics based on experimental data. On the basis of research results on animals, the energy efficiencies of multilegged robots have been greatly increased.

The total COT is a commonly-used metric for evaluating the energy efficiencies of animals and legged robots, which is written as

$$COT = P/Wv, \tag{6}$$

where P , W , and v are the robot’s power, weight, and speed, respectively [21]. The energy efficiencies of most multilegged robots are still worse than their biological counterparts, as seen in Figure 21. For instance, the COT of the BigDog quadruped robot ($COT = 15$) is significantly higher than animals of similar mass. In fact, the conversion of electricity to mechanical energy is much more efficient than the conversion of biological energy to mechanical energy. Thus, it is possible for robot designs to produce inefficiencies. To improve energy efficiency, passive dynamics have been employed to design legged robots, such as the Ranger robot from Cornell University [161]. Although it obtained very high energy efficiency ($COT = 0.19$), the Ranger sacrificed agility to maximize the passive dynamics. Legged robots with



more versatility, such as BigDog and ASIMO, are much less efficient than animals of similar scale. Series elastic elements have also been adopted to improve energy efficiency. For example, the StarLETH [20] and ANYmal [10] robots obtained COTs of 1.7 and 1.2, respectively, by employing SEA actuators. There exist three major energy losses, namely, heat losses of actuators, transmission losses, and interaction losses with the environment. To reduce these losses, Seok et al. [22] adopted a motor with a large gap radius, a regenerative driver, and a low inertia leg to design the Cheetah series robots. The Cheetah robots obtained very low COTs, rivaling running animals with similar masses [23, 25].

6.4 Software Architecture

The multilegged robot is a typical MMM robotic system, and its software computing architecture is very complicated. The hierarchical control architecture is usually adopted for the control of multilegged robots. A typical tiered control architecture consists of high-level and low-level controllers, as seen in Figure 22 [114]. The high-level controller includes a gait pattern modulator and a leg-trajectory generator. The former imposes an intended gait-pattern on the gait pattern modulator, and the latter offers a designed foot-end trajectory to the low-level controller, i.e., the leg controller. The leg controller realizes virtual leg compliance through active impedance control [162] or proprioceptive impedance control [114]. In the hierarchical architecture, low-level control operates at much higher frequencies than high-level control. For instance, the real-time whole-body controller of the ANYmal robot is timed by the CAN driver, which communicates with the actuator units at 400 Hz. However, the commands are exchanged to a less time-critical foothold planner through the robot operating system (ROS) [10]. This architecture makes it easier to expand

computing resources for future sensing, planning, and navigation [25].

There are two basic hypotheses [112] for this tiered control architecture. First, the continuous self-stabilizing task of dynamic locomotion can be achieved by planning the compliance of the virtual leg. Second, owing to the equilibrium-point hypothesis [163], the modulation of ground reaction force can be adjusted by designing the foot-end trajectories of the stance phase. Thus, the contact force control can be effectively achieved by penetrating the equilibrium position of the impedance control to the ground surface. The most significant advantage of the tiered control framework is that it has fewer control parameters such as gait-patterns, locomotion speed, and foot-end trajectories. Furthermore, all control parameters except the virtual ground-penetration depth can be predetermined by preliminary experiments. The Cheetah 1 robot using this kind of control model with fixed control parameters can yield self-stabilizing trot-running at speeds up to 6 m/s [113].

7 Future Research

In the above sections, the mechanism, actuation, perception, and control of highly dynamic multilegged robots are surveyed, and many important research results are presented. From this review, key topics for future research on multilegged robots can be determined as follows.

7.1 Mechanism and Actuation

In terms of mechanisms, bionic inspiration is still the primary basis for design. There are three detailed factors for design, namely actuation–transmission decoupling, serial–parallel coupling, and rigid–flexible coupling, as seen in Figure 23. Actuation–transmission decoupling yields the low inertia leg and makes it easy for electrical actuation devices to be protected from harsh environments. For a leg mechanism with serial–parallel hybrid topology, the serial module enlarges the foot-end workspace while the parallel module increases the stiffness. The rigid–flexible coupling mechanism has the greatest ability to handle uncertainties or disturbances like contact collisions.

In terms of actuation, there exist QDD, SEA, and hydraulic actuation methods, which can meet the basic actuating requirements of highly dynamic multilegged robots. However, actuation dynamics must be modeled more precisely in the future, a process that depends on attaining accurate physical parameters or force compensation algorithms. Physical parameters can be identified by both experimental and simulation methods. For instance, reinforcement learning is an effective method to determine control parameters of actuation dynamics.

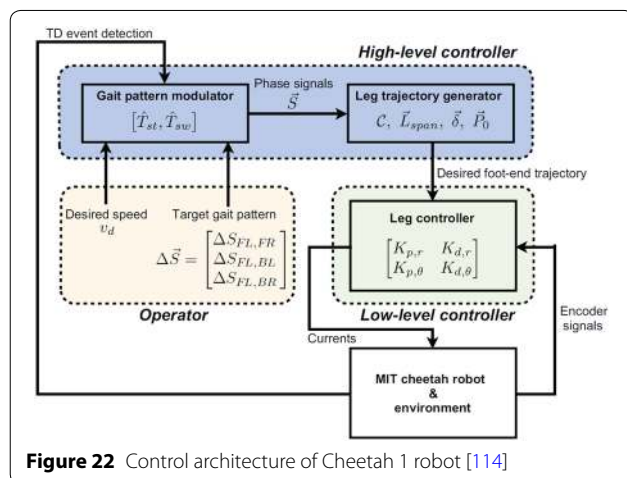


Figure 22 Control architecture of Cheetah 1 robot [114]

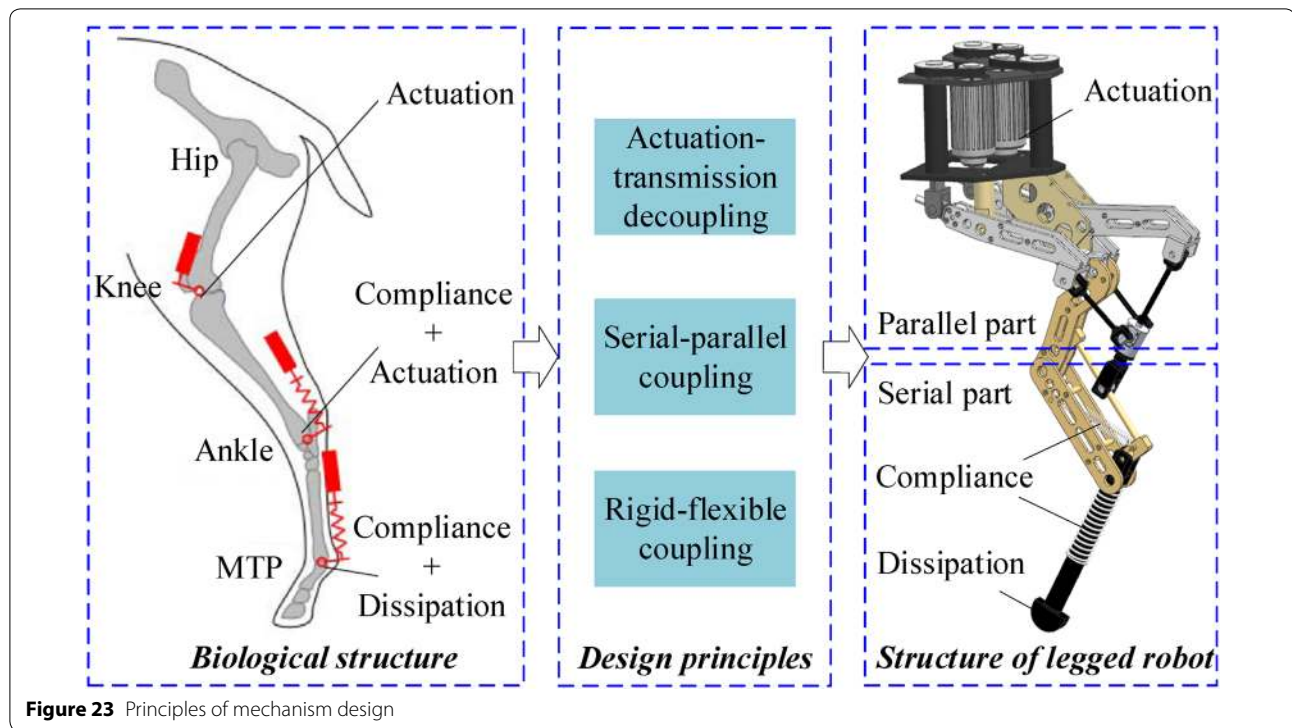


Figure 23 Principles of mechanism design

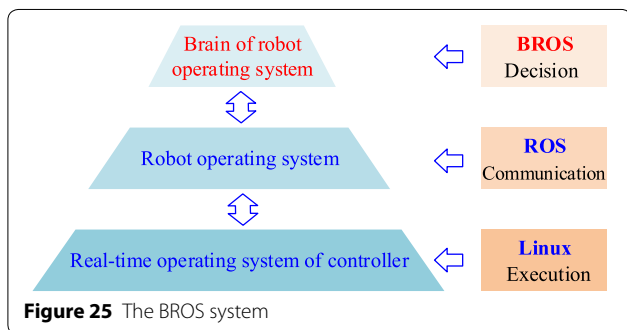
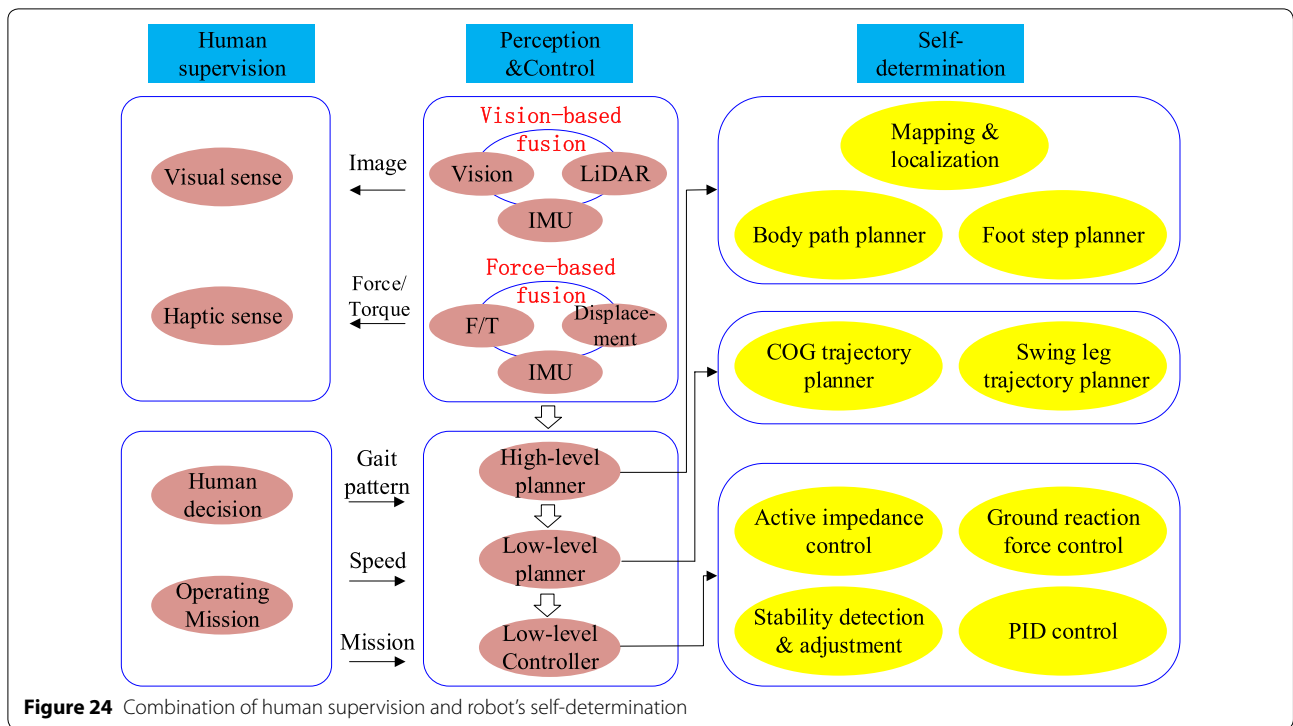
Because there exist time delays between force measurement and dynamic response in the actuation process, output torque error will inevitably be produced. For simple actuators such as QDD, the delay model can be derived, and thus the output error can be easily eliminated by model-based force compensation. However, for complex actuators, such as SEA and hydraulic cylinders commonly used in large-scale legged robots, the models of force measurement delay and dynamic response, and the stiffness and damping of the actuators are all unknown. Therefore, the force compensation of complex actuators is still a challenging issue for highly dynamic multilegged robots.

7.2 Perception and Control

In terms of perception, there are two important aspects that need to be further studied for highly dynamic multilegged robots, i.e., the improvement of adaptability and multisensor fusion. Regarding the first aspect, the perception algorithms used for other mobile robots like wheeled or tracked robots cannot be directly used for multilegged robots. For instance, a legged robot should have the ability to step on, step over, or bypass obstacles, which requires a map containing detailed geometric features of the local terrain. However, few works concerning wheeled or tracked robots establish such maps. Regarding the second aspect, multisensor fusion includes not only the fusion of multiple exteroceptive sensors, such as

LiDAR and a stereo camera but also the fusion between exteroceptive and proprioceptive sensors. For example, the fusion of measurements from IMU with 3D leg odometry and 3D visual odometry measurements from 3D vision can be used for robust pose estimation of multilegged robots in harsh outdoor environments. The computation of leg odometry is based on a forward kinematic model, which needs measurements from proprioceptive sensors such as joint encoders.

In terms of control, there are two important conclusions. First, the combination of the self-determination of the multilegged robot and human supervision is still the key to a breakthrough for the legged robot to perform complex missions (Figure 24). The current state of multilegged robots' technologies cannot meet the requirements for performing complex tasks in harsh outdoor environments. The human-in-the-loop control mode is a better choice for multilegged robots. The legged robot obtains necessary information via fusion perception such as vision-based and force-based fusion perception. This information is used for both control planning of the multilegged robot and human decision-making. The operator will give orders to the multilegged robot according to visual and haptic sensing. The control system of the legged robot consists of a high-level planner, low-level planner, and low-level controller, which autonomously carry out mapping and localization, trajectory planning, active impedance control, and so on.

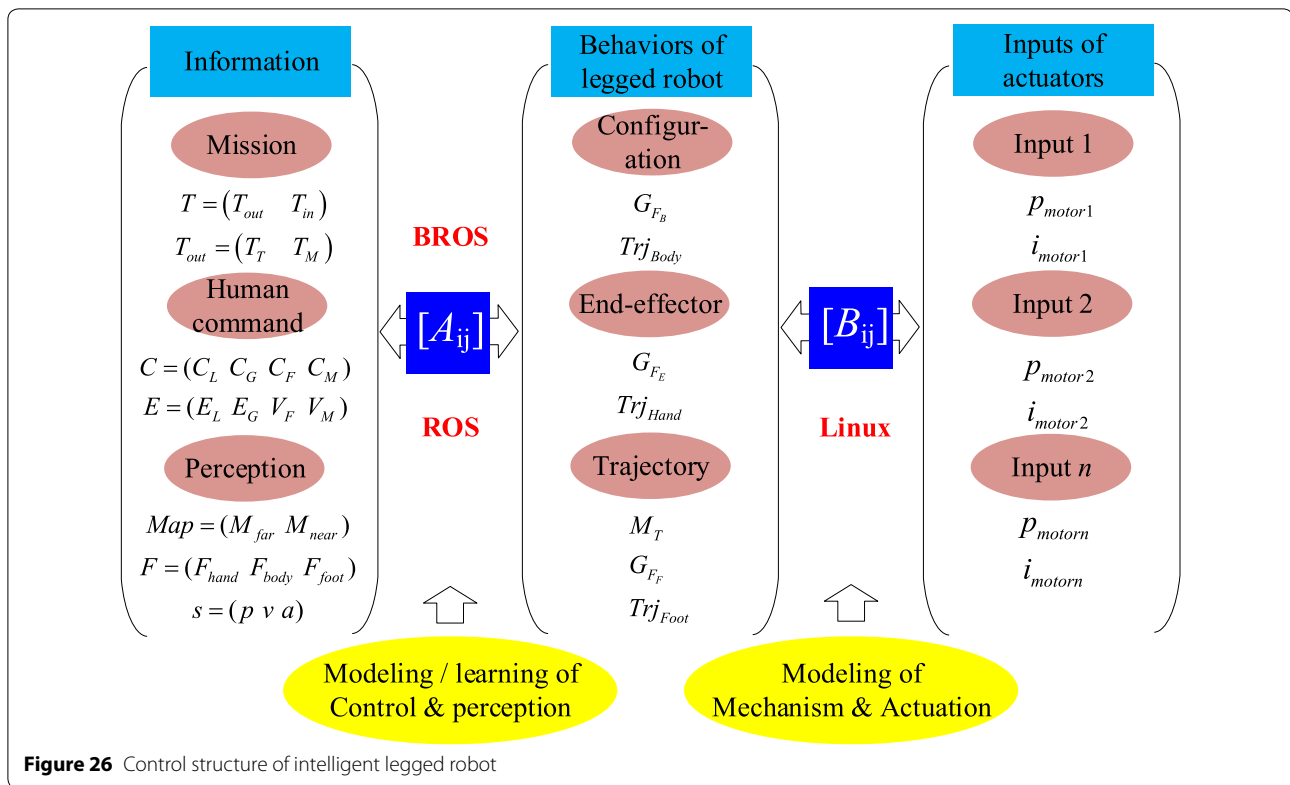


Second, it is believed that the conventional control architecture will not meet the requirements of future intelligent legged robots. The traditional architecture consists of communication and execution layers, which can be realized by the robot operating system (ROS) and the real-time operating system of the controller, such as Linux, as seen in Figure 25. There are three types of information for the legged robot, i.e., the mission (such as manipulating), human commands, and perception. The behaviors of legged robots consist of the configuration of the whole body as well as the motion characteristics and trajectory characteristics of all end-effectors of the torso and legs. Traditionally, the legged robot obtains its behaviors by information modeling according to methods mentioned in Sections 5 and 6. The

ROS realizes communication between the information and the behaviors. Then the input of actuation can be achieved according to kinematic and dynamic models of legged mechanisms and the actuators. The controller equipped with a real-time operating system, such as Linux enables communication between the behaviors and the inputs. The whole process is shown in Figure 26. However, with the development of artificial intelligence, some novel control methods such as RL have been used to improve the dynamic performance of multilegged robots. Therefore, it is vital to the development of legged robots to establish a new decision layer in the ROS and Linux, which is called the brain of ROS (BROS, see Figures 25, 26). The BROS is employed to establish the relationship between the information and the behaviors. First, the description and classification of behaviors of multilegged robots must be studied, and then the databases of configurations, motion, and trajectory characteristics can be established. Second, the description and classification of each kind of information need to be proposed, which can form logic mapping from information to behaviors.

8 Conclusions

In recent years, multilegged robots have achieved impressive advancements in dynamic performance. However, they are still far from being significantly versatile and robust. This paper addressed major points



that might lead to breakthroughs for multilegged robots.

- (1) Twenty-one typical multilegged robots were surveyed, and the most appealing performances of these robots were presented. It was noted that some quadruped robots have recently entered the market, which might help meet real commercial requirements and promote the development of key technologies.
- (2) The commonly used serial and parallel configurations of leg mechanisms were described and classified. The latest transmission structures and rigid-flexible coupling structures were also presented.
- (3) Three types of actuators—namely, hydraulic, QDD, and SEA actuators—were analyzed. Since actuation has a significant impact on many aspects of multilegged robots, this paper devoted special attention to the three important functions of actuation: high robustness against impacts, accurate velocity control, and low-impedance force control.
- (4) Sensors and modeling methods used for perception were reviewed. Studies concerning the mapping and localization abilities of multilegged robots were surveyed.

- (5) Control methods were presented in terms of gait pattern, control strategy, energy efficiency, and software architecture. The control of highly dynamic multilegged robots is another significant challenge, and thus this paper paid particular attention to the development trends of control strategies. Four dynamics-based control methods and two model-free control methods were illustrated in detail.

Although great research progress has been achieved in the field of multilegged robots, there are many significant problems that need to be further studied.

- (1) Novel mechanisms with serial-parallel coupling, rigid-flexible coupling, and actuation-transmission decoupling topologies must be synthesized. Actuation dynamics must be modeled more precisely in the future.
- (2) The adaptability improvement of perception modeling and multisensor fusion are still open issues. Control models with a combination of robot self-determination and human supervision as well as control architectures with the BROS system need further study.

Acknowledgements

Not applicable.

Authors' Contributions

JH was in charge of the whole data analysis; JH and FG wrote the manuscript. All authors read and approved the final manuscript.

Authors' Information

Jun He, born in 1981, is currently an associate professor at *State Key Laboratory of Mechanical System and Vibration, Shanghai Jiaotong University, China*. He received his doctoral degree from *Shanghai Jiaotong University, China*, in 2009. His research interests include mechanism and robotics in space.

Feng Gao, born in 1956, is currently a professor at *State Key Laboratory of Mechanical System and Vibration, Shanghai Jiaotong University, China*. He received his doctoral degree in *Beihang University, China*, in 1991.

Funding

Supported by National Natural Science Foundation of China (Grant Nos. 51575337, U1613208), Equipment Pre-research Aerospace Joint Fund (Grant No. 6141B06220407), Key Laboratory Fund of Science and Technology on Space Intelligent Control (Grant No. HTKJ2019KL502011).

Competing Interests

The authors declare no competing financial interests.

Received: 20 April 2020 Revised: 11 August 2020 Accepted: 10 September 2020

Published online: 09 November 2020

References

- [1] H W Park, P Wensing, S Kim. Online planning for autonomous running jumps over obstacles in high-speed quadrupeds. *Proceedings of Robotics: Science and Systems*, 2015: 2330–2337.
- [2] H W Park, M Y Chuah, S Kim. Quadruped bounding control with variable duty cycle via vertical impulse scaling. *The 2014 IEEE/RSJ International Conference on Intelligent Robots and Systems*, 2014: 3245–3252.
- [3] J Hwangbo, J Lee, A Dosovitskiy, et al. Learning agile and dynamic motor skills for legged robots. *Science Robotics*, 2019, 4(26): eaau5872.
- [4] H Shim, B H Jun, H Kang, et al. Development of underwater robotic arm and leg for seabed robot. *OCEANS-Bergen, 2013 MTS/IEEE*, 2013: 6608167.
- [5] K Nagatani, S Kiribayashi, Y Okada, et al. Emergency response to the nuclear accident at the Fukushima Daiichi nuclear power plants using mobile rescue robots. *Journal of Robotic Systems*, 2013, 30(1): 44–63.
- [6] Qiao Sun, Feng Gao, Xianbao Chen. Towards dynamic alternating tripod trotting of a pony-sized hexapod robot for disaster rescuing based on multi-modal impedance control. *Robotica International Journal of Information Education & Research in robotics & Artificial Intelligence*, 2018, 36: 1048–1076.
- [7] Yuan Tian, Feng Gao. Efficient motion generation for a six-legged robot walking on irregular terrain via integrated foothold selection and optimization-based whole-body planning. *Robotica International Journal of Information Education & Research in Robotics & Artificial Intelligence*, 2018, 36: 333–352.
- [8] Zhijun Chen, Feng Gao, Qiao Sun, et al. Ball-on-plate motion planning for six-parallel-legged robots walking on irregular terrains using pure haptic information. *Mechanism and Machine Theory*, 2019, 141: 136–150.
- [9] A Norton, W Ober, L Baraniecki, et al. Analysis of human–robot interaction at the DARPA Robotics Challenge Finals. *International Journal of Robotics Research*, 2017, 36: 483–513.
- [10] M Hutter, C Gehring, D Jud, et al. ANYmal—a highly mobile and dynamic quadrupedal robot. *IEEE/RSJ International Conference on Intelligent Robots and Systems*, 2016: 38–44.
- [11] C Semini, V Barasuol, J Goldsmith, et al. Design of the hydraulically actuated, torque-controlled quadruped robot HyQ2Max. *IEEE/ASME Transactions on Mechatronics*, 2017, 22: 635–646.
- [12] Machado J A Tenreiro, M Silva. An overview of legged robots. *MME 2006 - International Symposium on Mathematical Methods in Engineering*, 2006: 1–38.
- [13] Hongchao Zhuang, Haibo Gao, Zongquan Deng, et al. A review of heavy-duty legged robots. *Science China Technological Science*, 2014, 57: 298–314.
- [14] Xiangrui Meng, Shuo Wang, Zhiqiang Cao, et al. A review of quadruped robots and environment perception. *Proceedings of the 35th Chinese Control Conference*, 2016: 6350–6356.
- [15] C Semini, J Goldsmith, B U Rehman, et al. Design overview of the hydraulic quadruped robots HyQ2Max and HyQ2Centaur. *The Fourteenth Scandinavian International Conference on Fluid Power*, 2015: 20–22.
- [16] N Deshpande, J Ortiz, I Sarakoglou, et al. Next-generation collaborative robotic systems for industrial safety and health. *SAFE 2017, Safety and Security Engineering VII*, 2017: 187–200.
- [17] V Barasuol, J Buchli, C Semini, et al. A reactive controller framework for quadrupedal locomotion on challenging terrain. *IEEE International Conference on Robotics & Automation*, 2013: 2554–2561.
- [18] A Winkler, C Mastalli, I Havoutis, et al. Planning and execution of dynamic whole-body locomotion for a hydraulic quadruped on challenging terrain. *IEEE International Conference on Robotics & Automation*, 2015: 5148–5154.
- [19] C Semini, J Goldsmith, D Manfredi, et al. Additive manufacturing for agile legged robots with hydraulic actuation. *IEEE International Conference on Advanced Robotics*, 2015: 123–129.
- [20] M Hutter, C Gehring, M A Hopfner, et al. Toward combining speed, efficiency, versatility, and robustness in an autonomous quadruped. *IEEE Transaction on Robotics*, 2014, 30: 1427–1440.
- [21] V A Tucker. The energetic cost of moving about: Walking and running are extremely inefficient forms of locomotion, much greater efficiency is achieved by birds, fish and bicyclists. *American Scientist*, 1975, 63(4): 413–419.
- [22] S Seok, A Wang, M Y Chuah, et al. Design principles for highly efficient quadrupeds and implementation on the MIT cheetah robot. *2013 IEEE International Conference on Robotics and Automation* 2013: 3307–3312.
- [23] H W Park, P Wensing, S Kim. High-speed bounding with the MIT Cheetah 2: Control design and experiments. *The International Journal of Robotics Research*, 2017: 167–192.
- [24] G A Folkertsma, S Kim, S Stramigioli. Parallel stiffness in a bounding quadruped with flexible spine. *2012 IEEE/RSJ International Conference on Intelligent Robots and Systems*, 2012: 2210–2215.
- [25] G Bledt, M Powell, B Katz. MIT Cheetah 3: design and control of a robust, Dynamic Quadruped Robot. *2018 IEEE/RSJ International Conference of Intelligent Robots and Systems*, 2018: 2245–2252.
- [26] Hui Chai. *Research and implementation on compliance and force control of hydraulically actuated quadruped robot*. Jinan: Shandong University, 2016: 15–18. (in Chinese)
- [27] Zhenyu Jiang. *Control of quadruped robot in trotting gait based on SLIP model*. Harbin: Harbin Institute of Technology, 2014: 79–85. (in Chinese)
- [28] Xianbao Chen, Feng Gao, Chenkun Qi, et al. Spring parameters design for the new hydraulic actuated quadruped robot. *Journal of Mechanisms & Robotics*, 2014, 6(2): 021003.
- [29] Huixiang Xie. *Intuitive Control Based on Virtual Model for Quadruped Robot Trot Gait*. Changsha: National University of Defense Technology, 2015: 100–102. (in Chinese)
- [30] A Rönnau, G Heppner, M Nowicki, et al. LAURON V: A versatile six-legged walking robot with advanced maneuverability. *IEEE/ASME International Conference on Advanced Intelligent Mechatronics*, 2014: 82–87.
- [31] A Roennau, G Heppner, M Nowicki, et al. Reactive posture behaviors for stable legged locomotion over steep inclines and large obstacles. *IEEE/RSJ International Conference on Intelligent Robots and Systems*, 2014: 4888–4894.
- [32] H Kang, H Shim, B H Jun, et al. Design of the underwater link-joint system for the multi-legged underwater robot "CR200". *Proceedings of the MTS/IEEE OCEANS 2012 Yeosu*, 2012: 1–6.
- [33] H Shim, B H Jun, H Kang, et al. Development of underwater robotic arm and leg for seabed robot, CRABSTER200. In: *Proceedings of the MTS/IEEE OCEANS 2013 Bergen*, 2013: 1–6.
- [34] Yang Pan, Feng Gao. Leg kinematic analysis and prototype experiments of walking-operating multifunctional hexapod robot. *Proceedings of*

- the Institution of Mechanical Engineers, Part C: Journal of Mechanical Engineering Science*, 2014, 228(12): 2217–2232.
- [35] Hongchao Zhuang. *Electrically driven large-load-ratio six-legged robot structural design and its mobile characteristics research*. Harbin: Harbin Institute of Technology, 2014: 126–128. (in Chinese)
- [36] Jun He, Feng Gao. Type synthesis for bionic quadruped walking robots. *Journal of Bionic Engineering*, 2015, 12: 527–538.
- [37] S Seok, A Wang, D Otten, et al. Actuator design for high force proprioceptive control in fast legged locomotion. In: *2012 IEEE/RSJ International Conference on Intelligent Robots and Systems*, Vilamoura, 2012: 1970–1975.
- [38] H Witte, R Hackert, W Ilg, et al. Quadrupedal mammals as paragons for walking machines. In: *Proc AMAM – Adaptive Motion in Animals and Machines*, 2003: TuA-II-2.1–TuA-II-2.4.
- [39] Fischer, R Blickhan. The tri-segmented limbs of therian mammals: kinematics, dynamics, and self-stabilization—A review. *Journal of Experimental Zoology, Part A, Comparative Experimental Biology*, 2006, 305(11): 935–952.
- [40] A Spröwitz, A Tuleu, M Vespignani, et al. Towards dynamic trot gait locomotion: Design, control, and experiments with Cheetah-cub, a compliant quadruped robot. *The International Journal of Robotics Research*, 2013, 32(8): 932–950.
- [41] M H Raibert, M Chepponis, H J Benjamin. Running on four legs as though they were one. *IEEE Journal of Robotics and Automation*, 1986, 2: 70–82.
- [42] I Poulakakis, E Papadopoulos, M Buehler. On the stability of the passive dynamics of quadrupedal running with a bounding gait. *The International Journal of Robotics Research*, 2006, 25: 669–687.
- [43] J Estremera, K J Waldron. Thrust control, stabilization and energetics of a quadruped running robot. *The International Journal of Robotics Research*, 2008, 27(10): 1135–1151.
- [44] H Marco, C D Remy, A H Mark, et al. High compliant series elastic actuation for the robotic leg ScarLETH. In: *Proc. International Conference Climbing Walking Robots*, 2011: 507–514.
- [45] L D Maes, M Herbin, R Hackert, et al. Steady locomotion in dogs: temporal and associated spatial coordination patterns and the effect of speed. *Journal of Experimental Biology*, 2008, 211(1): 138–149.
- [46] R M Walter, D R Carrier. Ground forces applied by galloping dogs. *Journal of Experimental Biology*, 2007, 210(2): 208–216.
- [47] M Raibert, K Blankespoor, G Nelson, et al. The rough-terrain quadruped robot. In: *Proceedings of the 17th World Congress*, 2008: 10823–10825.
- [48] C Semini, N G Tzagarakis, E Guglielmino, et al. Design of HyQ - a hydraulically and electrically actuated quadruped robot. *Proceedings of the Institution of Mechanical Engineers. Part I: Journal of Systems and Control Engineering*, 2011, 225: 1–19.
- [49] T C Boaventura. *Hydraulic compliance control of the quadruped robot HyQ*. Genoa: University of Genoa, Italy and Istituto Italiano di Tecnologia (IIT), 2013.
- [50] B U Rehman, M Focchi, M Frigerio, et al. Design of a hydraulically actuated arm for a quadruped robot. *Proceedings of the International Conference on Climbing and Walking Robots (CLAWAR)*, 2015: 1–8.
- [51] Mattila, J Koivumaki, D G Caldwell, et al. A survey on control of hydraulic robotic manipulators with projection to future trends. *IEEE/ASME Transactions on Mechatronics*, 2017, 22(2): 669–680.
- [52] Jing Wang. *Research on new hydraulic and pneumatic actuation for robots*. Shanghai: Shanghai Jiao Tong University, 2011. (in Chinese)
- [53] G Benjamin Katz. *A low cost modular actuator for dynamic robots*. Boston: MIT, 2018.
- [54] H W Park, S Park, S Kim. Variable-speed quadrupedal bounding using impulse planning: Untethered high-speed 3D Running of MIT Cheetah 2. In: *2015 IEEE International Conference on Robotics and Automation (ICRA)*, 2015: 5163–5170.
- [55] C R Carignan, K R Cleary. Closed-loop force control for haptic simulation of virtual environments [OL]. *Haptics-e*, 2000, 1(2): 1–14 [2000-02-23]. <http://www.haptics-e.org>.
- [56] K Gavin, A De Avik, D E Koditschek. Design principles for a family of direct-drive legged robots. *IEEE Robotics and Automation Letters*, 2016, 1(2): 900–907.
- [57] S Seok, A Wang, Otten D, et al. Actuator design for high force proprioceptive control in fast legged locomotion. *2012 IEEE/RSJ International Conference on Intelligent Robots and Systems*, 2012: 1970–1975.
- [58] J E Pratt, B T Krupp. Series elastic actuators for legged robots. *Proceedings of SPIE - The International Society for Optical Engineering*, 2004, 5422: 135–144.
- [59] P Henry, M Krainin, E Herbst, et al. RGB-D mapping: Using Kinect-style depth cameras for dense 3D modeling of indoor environments. *The International Journal of Robotics Research*, 2012, 31(5): 647–663.
- [60] A Howard. Real-time stereo visual odometry for autonomous ground vehicles. In: *Proceedings of the 2008 IEEE/RSJ International Conference on intelligent robots and systems (IROS)*, 2008: 3946–3952.
- [61] A Mohamed. *Robust real-time visual odometry for autonomous ground vehicles*. Dearborn: University of Michigan, 2017.
- [62] K Cho, S H Baeg, S Park. 3D pose and target position estimation for a quadruped walking robot. *International Conference on Ubiquitous Robots and Ambient Intelligence*, 2013: 466–467.
- [63] S Bazeille, V Barasuol, M Focchi, et al. Quadruped robot trotting over irregular terrain assisted by stereo-vision. *Intelligent Service Robotics*, 2014, 7(2):67–77.
- [64] A Chilian, H Hirschmuller, M Gornor, et al. Multisensor data fusion for robust pose estimation of a six-legged walking robot. *IEEE/RSJ International Conference on Intelligent Robots and Systems*, 2011: 2497–2504.
- [65] J S Gutmann, M Fukuchi, M Fujita, et al. A floor and obstacle height map for 3D navigation of a humanoid robot. *Proceedings of the 2005 IEEE International Conference on Robotics and Automation*, 2005: 1066–1071.
- [66] I Rekleitis, J L Bedwani, E Dupuis, et al. Autonomous over-the-horizon navigation using LIDAR data. *Autonomous Robots*, 2013, 34(1): 1–18.
- [67] G Ishigami, M Otsuki, T Kubota. Range-dependent Terrain mapping and multi-path planning using cylindrical coordinates for a planetary exploration rover. *Journal of Field Robotics*, 2013, 30(4): 536–551.
- [68] S Khan, A Dometios, C Verginis, et al. Rmap: a rectangular cuboid approximation framework for 3D environment mapping. *Autonomous Robots*, 2014, 37(3): 261–277.
- [69] Xun Chai, Feng Gao, Chenkun Qi, et al. Obstacle avoidance for a hexapod robot in unknown environment. *Science China- Technological Sciences*, 2017, 60(6): 818–831.
- [70] H Durrantwhyte, T S Bailey. Simultaneous localization and mapping: part I. *IEEE Robotics and Automation Magazine*, 2006, 13(2): 99–110.
- [71] S Thrun, Y Liu, D Koller, et al. Simultaneous localization and mapping with sparse extended information filters. *The International Journal of Robotics Research*, 2004, 23(7–8): 693–716.
- [72] M Montemerlo, S Thrun, D Koller, et al. Fast-SLAM: A factored solution to the simultaneous localization and mapping problem. *National Conference on Artificial Intelligence*, 2002: 593–598.
- [73] S J Julier, J K Uhlmann. Unscented filtering and nonlinear estimation. *Proceedings of the IEEE*, 2004, 92(3): 401–422.
- [74] S Thrun, M Montemerlo. The graph SLAM algorithm with applications to large-scale mapping of urban structures. *The International Journal of Robotics Research*, 2006, 25(5): 403–429.
- [75] A J Davison, I Reid, N D Molton, et al. MonoSLAM: Real-time single camera SLAM. *IEEE Transactions on Pattern Analysis and Machine Intelligence*, 2007, 29(6): 1052–1067.
- [76] Danping Zou, Ping Tan. CoSLAM: Collaborative visual SLAM in dynamic environments. *IEEE Transactions on Pattern Analysis and Machine Intelligence*, 2013, 35(2): 354–366.
- [77] T S Bailey, H Durrantwhyte. Simultaneous localization and mapping (SLAM): part II. *IEEE Robotics and Automation Magazine*, 2006, 13(3): 108–117.
- [78] R M Alexander. The gaits of bipedal and quadrupedal animals. *The International Journal of Robotics Research*, 1984, 3(2): 49–59.
- [79] S Coros, A Karpathy, B Jones, et al. Locomotion skills for simulated quadrupeds. *The International Conference on Computer Graphics and Interactive Techniques*, 2011, 30(4): 59.
- [80] D Graham. Pattern and control of walking in insects. *Advances in Insect Physiology*, 1985: 31–140.
- [81] C L Vaughan, M Omalley. Froude and the contribution of naval architecture to our understanding of bipedal locomotion. *Gait and Posture*, 2005, 21(3): 350–362.
- [82] R J Full, R Blickhan, L H Ting, et al. Leg design in hexapedal runners. *The Journal of Experimental Biology*, 1991, 158(1): 369–390.

- [83] R J Full. Concepts of efficiency and economy in land locomotion. In: *Efficiency and Economy in Animal Physiology*. New York: Cambridge University Press, 1990.
- [84] M H Raibert, M Chepponis, H B Brown, et al. Running on four legs as though they were one. *IEEE Transaction on Robotics and Automation*, 1986, 2(2): 70–82.
- [85] M H Raibert. Trotting, pacing and bounding by a quadruped robot. *Journal of Biomechanics*, 1990: 79–98.
- [86] J G Cham, J K Karpick, M R Cutkosky. Stride period adaptation of a biomimetic running hexapod. *The International Journal of Robotics Research*, 2004, 23(2): 141–153.
- [87] C D Bellicoso, C Gehring, J Hwangbo, et al. Perception-less terrain adaptation through whole body control and hierarchical optimization. *IEEE-RAS International Conference on Humanoid Robots*, 2016: 558–564.
- [88] Tsutian Lee, Chingming Liao, Tingkou Chen. On the stability properties of hexapod tripod gait. *IEEE Journal on Robotics and Automation*, 1988, 4(4): 427–434.
- [89] M Vukobratovic, B Borovac. Zero-moment point: thirty-five years of its life. *International Journal of Humanoid Robotics*, 2004, 1(1): 157–173.
- [90] M Kalakrishnan, J Buchli, P Pastor, et al. Fast, robust quadruped locomotion over challenging terrain. *IEEE International Conference on Robotics and Automation*, 2010: 2665–2670.
- [91] Guiyang Xin, Hua Deng, Guoliang Zhong, et al. Gait and trajectory rolling planning for hexapod robot in complex environment. *Proceedings of the Asian Conference on Mechanism and Machine Science 2016 & The International Conference on Mechanism and Machine Science of China*, F, 2017, Springer Verlag.
- [92] D A Messuri, C A Klein. Automatic body regulation for maintaining stability of legged vehicle during rough terrain locomotion. *IEEE Journal on Robotics and Automation*, 1985, RA-1(3): 132–141.
- [93] P V Nagy, S Desa, W L Whittaker. Energy-based stability measures for reliable locomotion of statically stable walkers: Theory and application. *International Journal of Robotics Research*, 1994, 13(3): 272–287.
- [94] E G Papadopoulos, D A Rey. A new measure of tip over stability margin for mobile manipulators. *Proceedings of the IEEE International Conference on Robotics and Automation*, 1996, 4: 3111–3116.
- [95] Bensheng Lin, Shin-Min Song. Dynamic modelling, stability and energy efficiency of a quadrupedal walking machine. *Proceedings of the IEEE International Conference on Robotics and Automation*, 1993, 3: 367–373.
- [96] A De, D E Koditschek. Vertical hopper compositions for reflexive and feedback-stabilized quadrupedal bounding, pacing, prinking, and trotting. *International Journal of Robotics Research*, 2018, 37(7): 743–778.
- [97] I Poulakakis, E Papadopoulos, M Buehler. On the stability of the passive dynamics of quadrupedal running with a bounding gait. *International Journal of Robotics Research*, 2006, 25(7): 669–687.
- [98] J Pratt, C M Chew, A Torres, et al. Virtual model control: an intuitive approach for bipedal locomotion. *International Journal of Robotics Research*, 2001, 20(2): 129–143.
- [99] I Havoutis, C Semini, D G Caldwell. Virtual model control for quadrupedal trunk stabilization. *The 8th Annual Conference on Principles and Concepts of Legged Locomotion-Dynamic Walking 2013*, Pittsburgh, Pennsylvania, 2013.
- [100] J D Carlo, P M Wensing, B Katz, et al. Dynamic locomotion in the MIT Cheetah 3 through convex model-predictive control. *2018 IEEE/RSJ International Conference on Intelligent Robots and Systems (IROS)* Madrid, Spain, 2018: 7440–7447.
- [101] Q Nguyen, M J Powell, B Katz, et al. Optimized jumping on the MIT Cheetah 3 Robot. *Proceedings of the IEEE International Conference on Robotics and Automation*, Montreal, Canada, 2019: 7448–7454.
- [102] C Gehring, S Coros, M Hutter, et al. Control of dynamic gaits for a quadrupedal robot. *2013 IEEE International Conference on Robotics and Automation (ICRA)*, 2013: 3287–3292.
- [103] M Hutter, H Sommer, C Gehring, et al. Quadrupedal locomotion using hierarchical operational space control. *International Journal of Robotics Research*, 2014, 33(8): 1047–1062.
- [104] C Gehring, et al. An optimization-based approach to controlling agile motions for a quadruped robot. *IEEE Robotics & Automation Magazine*, 2016, 23(1): 34–43.
- [105] Y Fukuoka, H Kimura, AH Cohen. Adaptive dynamic walking of a quadruped robot on irregular terrain based on biological concepts. *International Journal of Robotics Research*, 2003, 22(3-4): 187–202.
- [106] Y Fukuoka, H Kimura. Dynamic locomotion of a biomorphic quadruped Tekken-robot using various gaits: walk, trot, free-gait and bound. *Applied Bionics and Biomechanics*, 2009, 6(1): 63–71.
- [107] H Kimura, Y Fukuoka, A Cohen. Adaptive dynamic walking of a quadruped robot on natural ground based on biological concepts. *International Journal of Robotics Research*, 2007, 26(5): 475–490.
- [108] Jiaqi Zhang, Feng Gao, Xiaolei Han, et al. Trot gait design and CPG method for a quadruped robot. *Journal of Bionic Engineering*, 2014, 11(1): 18–25.
- [109] Jie Tan, Tingnan Zhang, E Coumans, et al. Sim-to-real: learning agile locomotion for quadruped robots. *Proceedings of Robotics: Science and Systems*, 2018, arXiv:1804.10332.
- [110] Binpeng Xue, M Andrychowicz, W Zaremba, et al. Sim-to-real transfer of robotic control with dynamics randomization. *2018 IEEE International Conference on Robotics and Automation*, Brisbane, Australia, 2018: 3803–3810.
- [111] D Wettergreen, C Thorpe. Gait generation for legged robots. *Proceedings of the International Conference on Intelligent Robots and Systems*, NC, USA, 1992: 1413–1420.
- [112] D J Hyun, J Lee, S Park, et al. Implementation of trot-to-gallop transition and subsequent gallop on the MIT Cheetah I. *International Journal of Robotics Research*, 2016, 35(13): 1627–1650.
- [113] J Lee, D J Hyun, J Ahn, et al. On the dynamics of a quadruped robot model with impedance control: Self-stabilizing high speed trot-running and period-doubling bifurcations. *2014 IEEE/RSJ International Conference on Intelligent Robots and Systems (IROS 2014)*, 2014: 4907–4913.
- [114] D J Hyun, S Seok, J Lee, et al. High speed trot-running: Implementation of a hierarchical controller using proprioceptive impedance control on the MIT Cheetah. *International Journal of Robotics Research*, 2014, 33(11): 1417–1445.
- [115] G A Cavagna, N C Heglund, C R Taylor. Walking, running, and galloping: mechanical similarities between different animals. *Proceedings of an International Symposium*, T J Pedley, ed., New York, 1975: 111–125.
- [116] A Seyfarth, H Geyer, M Guenther, et al. A movement criterion for running. *Journal of Biomechanics*, 2002, 35: 649–655.
- [117] D W Marhefka, D E Orin, J P Schmiedeler, et al. Intelligent control of quadruped gallops. *IEEE-ASME Transactions on Mechatronics*, 2004, 8(4): 446–456.
- [118] Jian Tian, Chao Ma, Cheng Wei, et al. A smooth gait planning framework for quadruped robot based on virtual model control. *2019 IEEE International Conference on Robotics and Automation*, 2019: 398–410.
- [119] CM Chew, GA Pratt. Dynamic bipedal walking assisted by learning. *Robotica*, 2002, 20(5): 477–491.
- [120] K Edin, M Damir, K Zdenko. Hybrid compliance control for locomotion of electrically actuated quadruped robot. *International Journal of Humanoid Robotics*, 2019, 94(3–4): 537–563.
- [121] AW Winkler, C Mastalli, I Havoutis. Planning and execution of dynamic whole-body locomotion for a hydraulic quadruped on challenging terrain. *2015 IEEE International Conference on Robotics and Automation*, 2015: 5148–5154.
- [122] I Havoutis, C Semini, J Buchli, et al. Quadrupedal trotting with active compliance. *2013 IEEE International Conference on Mechatronics*, 2013: 610–616.
- [123] C Gehring, S Coros, M Hutter, et al. Control of dynamic gaits for a quadrupedal robot. *2013 IEEE International Conference on Robotics and Automation*, 2013: 3287–3292.
- [124] H Xie, M Ahmadi, J Shang, et al. An intuitive approach for quadruped robot trotting based on virtual model control. *Proceedings of the Institution of Mechanical Engineers* 2015, 229(4): 342–355.
- [125] Songyang Xin, R Orsolino, N Tsagarakis. Online relative footstep optimization for legged robots dynamic walking using discrete-time model predictive control. *2019 IEEE/RSJ International Conference on Intelligent Robots and Systems*, Macau, China, 2019: 513–520.
- [126] A Herdt, N Perrin, PB Wiebe. Walking without thinking about it. *2010 IEEE/RSJ International Conference on Intelligent Robots and Systems*, 2010: 190–195.
- [127] S Faraji. *A model-based control approach for locomotion of biped robots*. Lausanne: Ecole Polytechnique Federale de Lausanne, 2013.

- [128] D Dimitrov, A Sherikov, P B Wieber. A sparse model predictive control formulation for walking motion generation. *2011 IEEE/RSJ International Conference on Intelligent Robots and Systems*, 2011: 2292–2299.
- [129] Y Wang, S Boyd. Fast model predictive control using online optimization. *2010 IEEE Transactions on Control Systems Technology*, 2010,18(2): 267–278.
- [130] H J Ferreau, H G Bock, M Diehl. An online active set strategy to overcome the limitations of explicit MPC. *International Journal of Robust and Nonlinear Control*, 2008, 18(8): 816–830.
- [131] S Boyd, L Vandenberghe. *Convex optimization*. Cambridge: Cambridge University Press, 2004.
- [132] Y Wang, S Boyd. Fast model predictive control using online optimization. *IEEE Transactions on Control Systems Technology*, 2010, 18(2): 267–278.
- [133] A Domahidi, E Chu, S Boyd. ECOS: An SOCP solver for embedded systems. *European Control Conference*, 2013: 3071–3076.
- [134] H Ferreau, C Kirches, A Potschka, et al. qpOASES: A parametric active-set algorithm for quadratic programming. *Mathematical Programming Computation*, 2014, 6(4): 327–363.
- [135] L Sentis, O Khatib. Synthesis of whole-body behaviors through hierarchical control of behavioral primitives. *International Journal of Humanoid Robotics*, 2005, 2(4): 505–518.
- [136] L Sentis. *Synthesis and control of whole-body behaviors in humanoid systems*. California: Stanford University, 2007.
- [137] M Mistry, J Buchli, S Schaal. Inverse dynamics control of floating base systems using orthogonal decomposition. *2010 IEEE International Conference on Robotics and Automation*, 2010, 3: 3406–3412.
- [138] B Aceituno-Cabezas, C Mastalli, Hongkai Dai, et al. Simultaneous contact, gait, and motion planning for robust multilegged locomotion via mixed-integer convex optimization. *IEEE Robotics and Automation Letters*, 2017: 1–10.
- [139] CD Bellicoso, F Jenelten, C Gehring, et al. Dynamic locomotion through online nonlinear motion optimization for quadrupedal robots. *IEEE Robotics and Automation Letters*, 2018, 3(3): 2261–2268.
- [140] F Farshidian, E Jelavi, A W Winkler, et al. Robust whole-body motion control of legged robots. *International Conference on Intelligent Robots and Systems*, 2017: 4589–4596.
- [141] S Kuindersma, F Permenter, R Tedrake. An efficiently solvable quadratic program for stabilizing dynamic locomotion. *2014 IEEE International Conference on Robotics and Automation (ICRA)*, Hong Kong, China, 2014: 2589–2594.
- [142] A Herzog, N Rotella, S Mason, et al. Multi-contact interaction with hierarchical inverse dynamics and momentum trajectory generation. *The 10th Annual Conference on Principles and Concepts of Legged Locomotion. Proceedings of Dynamic Walking*, Columbus, Ohio, 2015: 21–24.
- [143] D Owaki, A Ishiguro. A quadruped robot exhibiting spontaneous gait transitions from walking to trotting to galloping. *Scientific Reports*, 2017, 7(1): 277.
- [144] H Geyer, H Hugh. A muscle-reflex model that encodes principles of legged mechanics produces human walking dynamics and muscle activities. *IEEE Transactions on Neural Systems and Rehabilitation Engineering*, 2010, 18(3): 263–273.
- [145] J Auke, I Biorobotics. Using robots to emulate and investigate agile locomotion. *Science*, 2014, 346(6206): 196–203.
- [146] G Endo, J Morimoto, T Matsubara, et al. Learning CPG-based biped locomotion with a policy gradient method: Application to a humanoid robot. *International Journal of Robotics Research*, 2008, 27(2): 213–228.
- [147] C S Park, J H Kim. Stable modifiable walking pattern algorithm with constrained optimized central pattern generator. *Advances in Intelligent Systems and Computing*, 2012, 208: 223–230.
- [148] Y Fukuoka, Y Habu, T Fukui. A simple rule for quadrupedal gait generation determined by leg loading feedback: a modeling study. *Scientific Reports*, 2015, 5: 8169.
- [149] M Ajalloeian, S Pouya, A Sproewitz, et al. Central pattern generators augmented with virtual model control for quadruped rough terrain locomotion. *2013 IEEE International Conference on Robotics and Automation (ICRA)*, Karlsruhe, Germany, 2013: 3321–3328.
- [150] A J Ijspeert, A Crespi, D Ryczko, et al. From swimming to walking with a salamander robot driven by a spinal cord model. *Science*, 2007, 315(5817): 1416–1420.
- [151] T P Lillicrap, J J Hunt, A Pritzel, et al. Continuous control with deep reinforcement learning. *Computer Science*, 2015, <http://arxiv.org/abs/1509.02971v2>.
- [152] J Schulman, F Wolski, P Dhariwal, et al. Proximal policy optimization algorithms. *Computer Research Repository*, 2017, <http://arxiv.org/abs/1707.06347>.
- [153] Yan Duan, Xi Chen, R Houhoof, et al. Benchmarking deep reinforcement learning for continuous control. *Proceedings of the 33rd International Conference on International Conference on Machine Learning ICML'16*, New York, USA, 2016, 48: 1329–1338.
- [154] S Levine, P Pastor, A Krizhevsky, et al. Learning handeye coordination for robotic grasping with deep learning and large-scale data collection. *International Journal of Robotics Research*, 2018: 421–436.
- [155] A Boeing, T Braunl. Leveraging multiple simulators for crossing the reality gap. *IEEE 2012 12th International Conference on Control Automation Robotics & Vision (ICARCV)*, Guangzhou, China, 2012: 1113–1119.
- [156] T Lee, F C Park. A geometric algorithm for robust multibody inertial parameter identification. *IEEE Robotics and Automation Letters*, 2018, 3(3): 2455–2462.
- [157] A Minetti, L Ardigo, E Reinach, et al. The relationship between mechanical work and energy expenditure of locomotion in horses. *Journal of Experimental Biology*, 1999, 202(17): 2329–2338.
- [158] R M Alexander. Energy-saving mechanisms in walking and running. *Journal of Experimental Biology*, 1991, 160(1): 55–69.
- [159] B K Ahlborn, R W Blake, W M Megill. Frequency tuning in animal locomotion. *Zoology*, 2006, 109(1): 43–53.
- [160] D F Hoyt, S J Wickler, D J Dutto, et al. What are the relations between mechanics, gait parameters, and energetics in terrestrial locomotion. *Journal of Experimental Zoology*, 2006, 305A(11): 912–922.
- [161] P Bhounsule, J Cortell, A Ruina. Design and control of ranger: An energy-efficient, dynamic walking robot. *CLAWAR 2012—Proceedings of the Fifteenth International Conference on Climbing and Walking Robots and the Support Technologies for Mobile Machines*, Baltimore, Maryland, USA, 2012: 441–448.
- [162] C Semini, V Barasuol, T Boaventura, et al. Towards versatile legged robots through active impedance control. *International Journal of Robotics Research*, 2015, 34(7): 1003–1020.
- [163] E Bizzi, N Hogan, F A Mussa-Ivaldi, et al. Does the nervous system use equilibrium-point control to guide single and multiple joint movements. *Behavioral and Brain Sciences*, 1992, 15(4): 603–613.